Evaluation of microRNA mechanisms involved in collagen matrix therapy for myocardial infarction

by

Hélène Chiarella-Redfern

This thesis is submitted to the Faculty of Graduate and Postdoctoral Studies in partial fulfillment of the requirements for the Degree of:

Master of Science in Cellular and Molecular Medicine

Department of Cellular and Molecular Medicine
Faculty of Medicine
University of Ottawa
Division of Cardiac Surgery
University of Ottawa Heart Institute

© Hélène Chiarella-Redfern, Ottawa, Canada, 2015

Abstract

Myocardial infarction (MI), a late-stage event of many cardiovascular diseases (CVD), results in cardiomyocyte death, myeloid cell recruitment to promote cellular debris removal and excessive cardiac remodeling affecting architecture and function, which can ultimately lead to heart failure. Currently, the use of biomaterials to intervene on the hostile post-MI environment and promote myocardial healing is being investigated to restore cardiac function. It has been shown that an injectable collagen matrix improves cardiac repair by altering macrophage polarization, reducing cell death and enhancing angiogenesis, leading to a reduction in infarct size and improved cardiac function when delivered at 3 hours post-MI. MicroRNAs (miRNA) "fine tune" gene expression by negatively regulating the translational output of target messenger RNA (mRNA). As such, miRNAs present interesting therapeutic opportunities for the treatment of MI. However, the delivery of miRNA mimics and/or inhibitors can be complicated by degradation and off target effects. The **objectives** of this thesis were to determine how the matrix may regulate endogenous miRNAs and to explore the biomaterial's ability to deliver therapeutic miRNAs. It was shown that matrix treatment of MI mouse hearts resulted in altered expression of 119 miRNAs, some of which had functions linked to the beneficial effects of matrix treatment. Of particular interest, miR-92a was down-regulated within the infarct and peri-infarct cardiac tissue 2 days after matrix treatment (delivered at 3-hours post-MI) compared to PBS treatment. In *in vitro* cultures, the matrix down-regulated miR-92a levels in macrophages but did not significantly alter miR-92a expression in endothelial cells, circulating angiogenic cells or fibroblasts. In addition, using an *in vitro* model system, it was shown that the matrix may have the potential to deliver functional therapeutic miRNAs to cells; however further experimental optimisation is required to confirm these results.

Therefore, collagen matrix treatment may be a promising approach to regulate and/or deliver miRNAs for protecting the myocardial environment and improving function of the infarcted heart.

Table of Contents

List of Figures

List of Tables

Abbreviations

Ago2	Protein Argonaute 2
APS	Ammonium Persulfate
AS	Aortic Stenosis
ASO	Antisense Oligonucleotides
BMDM	Bone Marrow Derived Macrophages
CAC	Circulating Angiogenic Cell
CVD	Cardiovascular Diseases
DIG	Digoxigenin
DMEM	Dulbecco's modification of Eagle's medium
EC	Endothelial Cell
ECM	Extracellular Matrix
EDC	1-Ethyl-3-(3-Dimethylaminopropyl) Carbodiimide
EDG1	Endothelial Differentiation Gene 1
EDTA	Ethylenediaminetetraacetic Acid
ERK	Extracellular-Signal-Regulated Kinases
EtOH	Ethanol
FBS	Fetal Bovine Serum
HCAECs	Human Coronary Artery Endothelial Cells
HIFs	Hypoxia-Induced Transcription Factors
HCV	Hepatitis C Virus
Itgα5	Integrin Subunit a5
ItgaV	Integrin Subunit αV
IR	Ischemia/Reperfusion

ISH	*In Situ* Hybridization
KLF2	Kruppel-Like Factor 2
LAD	Left Anterior Descending
Ldlr	Low Density Lipoprotein Receptor
LNA	Locked Nucleic Acids
LV	Left Ventricle
LXR	Liver X Receptor
MAPK	Mitogen-Activated Protein Kinase Kinase
MES	2(-N-Morpholino) Ethanesulfonic Acid
MI	Myocardial Infarction
miRNA	microRNA
MMK4	Mitogen-Activation Protein Kinase Kinase 4
MMP-2	Metalloprotease-2
mRNA	Messenger RNA
NHS	N-Hydroxysuccinimide
PBMCs	Peripheral Blood Mononuclear Cells
PBS	Phosphate Buffered Saline
PTEN	Phosphatase and Tensin Homologue
Rap-1b	Ras-Related Protein Rap-1b
RISC	RNA-Induced Silencing Complex
S1P1	Sphingosine-1-Phosphate Receptor 1
SDS-PAGE	Sodium Dodecyl Sulfate-Polyacrylamide Gel Electrophoresis
Spry1	Sprouty Homologue 1
SS	Shear Stress

TEMED	Tetramethyethylenediamine
TLR	Toll-Like Receptor
UNG	Uracil-N Glycoslyase
UTR	Untranslated Region
VEGF	Vascular Endothelial Growth Factor

Acknowledgments

This work would not have been possible without the guidance and support of many scientific advisors and colleagues. To my supervisor, Dr. Erik Suuronen, thank you for taking me on and allowing me to pursue my Master's project under your supervision and providing me with guidance from day one. I am extremely grateful for the multiple opportunities he provided me with, such as attending national and international cardiovascular and tissue engineering conferences. Participation in conferences has proven invaluable as they allowed me to interact with experts in my field regarding my research.

Additionally, I would like to extend gratitude to my co-supervisor Dr. Katey Rayner who I consider a mentor and was a great resource throughout my project. She was always available to share her expertise and advice which was paramount to the success of my research and professional development. I am truly grateful.

Special thanks are given to Dr. Brian McNeill, Dr. Denuja Karunakaran and Michele Geoffrion who were of equal help and whose knowledge, time and experience were vital to my success and the success of the project.

I would also like to thank my thesis committee members, Dr. Stephen Lee and Dr. Thomas Lagace. They have provided me with valuable advice which helped strengthen the overall direction of the project.

A final thank you to the numerous people I met while at the Heart Institute who made my Masters studies an amazing and enjoyable learning experience and to my family and friends who patiently helped and supported me during this challenging and rewarding experience.

Statement of Contribution

Dr. Erik Suuronen and Dr. Katey Rayner came up with the concept and design of the project. The animal work was organized by Nick Blackburn, while Richard Seymour performed the LAD ligations, Dr. Donna Padavan prepared the collagen matrix, and Dr. Ali Ahmadi injected the matrix. The miRNA microarray was performed at the Stem Core Facility at the Ottawa Hospital Research Institute and the statistical analysis was done by Alphonse Chu. The isolation of bone marrow-derived macrophages was done with the help of Michele Geoffrion and Dr. Denuja Karunakaran.

INTRODUCTION

1. Introduction

1.1 Myocardial Infarction and Cardiac Repair

Myocardial infarction (MI), an ultimate consequence of many cardiovascular diseases (CVD), is the most common cause of acute cardiac injury and a leading cause for hospitalization and death worldwide.[1, 2] During MI, the cessation of blood supply to an area of the myocardium leads to the rapid necrosis of cardiac myocytes. Cardiac healing and repair following myocardial ischemia is a complex process of three overlapping phases: the inflammatory, proliferation and maturation phases.[3-6] In the inflammatory phase cardiomyocyte apoptosis and necrosis triggers an inflammatory response which replaces cellular debris with granulation tissue.[3, 4] During the last two phases a microvascular network is formed and a rigid collagenous scar is produced to replace the damaged tissue, which is essential for maintaining structural integrity and preventing the left ventricle from rupturing.[3, 6]

1.1.1 Inflammatory Response

Infarct healing is initiated by the rapid but highly controlled recruitment and activation of neutrophils and monocytes, which is triggered by cytokine release from injured myocytes.[3, 7] When myeloid cells migrate into the ischemic tissue, this activates neurohormonal and intracellular signalling, which localizes the response.[7] Within the infarct, the recruited neutrophils and macrophages clear the cellular and matrix debris.[2] Once the cellular debris has been removed, activated macrophages release cytokines and growth factors leading to granulation tissue formation, angiogenesis and fibroblast proliferation.[6] It is important to note that macrophages are plastic cells that embrace different activation states and can polarize into either an M1 or M2 phenotype in response to different stimuli.[8-10] Specifically, M1 macrophages are pro-inflammatory

and have been linked to inflammation after MI whereas M2 macrophages are anti-inflammatory and reparative and have been implicated in MI healing.[8, 11, 12] The resolution of inflammation is dependent on the transition from the M1 to M2 macrophage phenotype, with accelerated transition rate and an increased M2-to-M1 ratio leading to the promotion of angiogenesis and reduction of infarct size and ventricular remodelling.[13, 14] Thus, cardiac healing involves the activation and polarization of macrophages for the induction and resolution of inflammation and the transition to scar formation.[2, 15, 16]

1.1.2 Neovascularization

Angiogenesis is a crucial process in wound healing as tissue function depends on adequate blood supply.[17] After MI, the hypoxic environment activates hypoxia-inducible factors (HIFs), which are transcription factors that regulate angiogenic growth factors required for neovessel formation, such as vascular endothelial growth factor (VEGF).[2, 17-19] Neovessels are an important component of granulation tissue and are required to provide essential nutrients and oxygen to cells involved in wound healing.[2] It is during the proliferative phase that large capillary networks and "mother vessels" are formed.[20, 21] Circulating angiogenic cells (CACs) play a role in cardiac repair through angiogenesis.[22] Upon infarction, they home to the site of cardiac injury where they may differentiate into endothelial cells and incorporate into neovessels.[23, 24] In addition, they release paracrine factors; the provision of these soluble factors is believed to be the primary mechanism through which CACs contribute to angiogenesis. Thus strategies to augment these angiogenic pathways to induce early reperfusion is important as it may reduce cardiac damage after MI by quickly returning oxygen and nutrients to the tissue.[7]

1.2 Rationale for Biomaterials

A major challenge for treating heart disease is the inability of the adult human heart to efficiently regenerate after cardiac stress.[2] Therapies to regenerate the myocardium and help restore function to the heart after MI are currently being heavily explored by researchers. Stem cell transplantation into the myocardium has emerged as a promising strategy to help regenerate the heart post-MI through the replacement of damaged tissue. Despite improving cardiac function, the benefit of this approach is limited due to poor cell survival and engraftment, and it also carries the potential risks of unwanted neoplastic growths if cells settle into non-target tissues.[25-27] Biomaterials, materials that interact with biological systems for medical purposes, can be used as vehicle for stem cell delivery. These have the potential to augment cell function, while improving engraftment and survival, and minimizing off-target cell delivery.[25, 28, 29] The therapeutic success of biomaterials in conjunction with cell therapies for the treatment of MI has well been documented.[30-33] Injectable materials are also therapeutically appealing as they can form to the defined size and shape of the cavity and may be delivered non-invasively.[34] In addition to their use for cellular delivery, biomaterials as stand-alone therapies (without cells) have also been shown to be beneficial for the treatment of MI.[35-37]

1.2.1 Collagen Matrices

Biomaterials can be classified as synthetic or natural, with natural biomaterials being derived from native extracellular matrix (ECM), such as collagen fibers.[29] Within the heart, the ECM provides structural support, interconnects cells and acts as an environment for cells to migrate and grow.[38] Cell-ECM interactions, which occur through surface adhesion molecules such as integrins, are extremely important as they initiate downstream signalling events that influence

cellular function. Studies delivering stem cells within an injectable matrix composed of ECM components into ischemic skeletal muscle have demonstrated improved cell persistence and regenerative effects.[39] Using ECM-like gels as therapeutic biomaterials is beneficial as they comprise components that are already found endogenously and are recognized by the cells, thus promoting more natural cellular behavior and minimizing the risk of initiating a negative immune response.[40] Collagen is the major ECM protein in the healthy heart, and is a frequently used as a biomaterial to treat cardiac injury due to its ability to recruit endogenous cells for regeneration and improve cardiac function.[29, 33, 41]

1.2.2 Functional Benefits of the Collagen Matrix

Collagen matrices have been shown to augment the angiogenic potential and proliferation of circulating angiogenic cells (CACs) *in vitro* and increase their mobilization after ischemic hindlimb injury *in vivo*.[42, 43] Improved arteriole density and perfusion was observed within ischemic tissue that received matrix treatment, highlighting its angiogenic potential.[42] Recently, the Suuronen lab showed that intramyocardial injections of a collagen matrix improved the post-MI cardiac environment. When the collagen matrix was injected into the infarcted tissue three hours after MI a number of functional benefits were observed in comparison to PBS-treated controls. Two days after matrix treatment, an increased ratio of M2:M1 macrophages was observed in the infarct, and at four weeks after injection significantly more capillaries and arterioles were observed in the infarcted tissue (unpublished, N. Blackburn). At 4 weeks, a significant reduction in infarct size and apoptosis was also observed in mice having received the therapeutic matrix, which preserved cardiac function up to three months post-MI (unpublished, N. Blackburn). Consequently, the collagen matrix shows promise as a treatment to mediate the post-MI

myocardial environment. However, how the collagen matrix improves cardiac function following MI remains unclear.

1.3 miRNA Biogenesis and Functional Concepts

MicroRNAs (miRNAs), a class of small non-coding RNAs, "fine tune" gene expression by negatively regulating the translational output of target messenger RNA (mRNA) in a sequence-dependent manner.[44-47] Most miRNA encoding genes are intergenic but can also be generated by the processing of introns of protein-coding genes allowing for the coordinated expression of a miRNA and protein, occasionally leading to the joint modulation of a biological process (ex: control of cholesterol homeostasis by miR-33 and its host gene).[48, 49] In mammals, the processing of miRNA encoding transcripts by Drosha-DGCR8 and Dicer leads to a miRNA duplex in which one strand is loaded into the RNA-induced silencing complex (RISC), becoming the "mature" miRNA and the other strand, called the star strand, is typically degraded (Figure 1.1).[46, 50] Once processed, mature miRNAs and pre-miRNAs can be selectively retained or released by a cell through packaging into microparticles (exosomes, microvesicles or apoptotic bodies) or associating with RNA-binding proteins, such as Ago2, possibly to regulate gene expression in distant target cells.[51-54] RISC coordinates the binding of the loaded miRNA to the 3' untranslated region (UTR) of target mRNA, which promotes mRNA degradation or translational inhibition, and thus reduces production of the protein.[45, 48] Most 3'UTRs contain potential binding sites for numerous miRNAs, allowing redundancy or cooperative interactions between various seemingly unrelated miRNAs.[45] In addition, miRNAs have been shown to regulate multiple genes governing the same biological processes (ex: the role of miR-29 in fibrosis) thus reducing the importance of single miRNA-mRNA interactions in eliciting a biological response.[55] The multi-target and multi-

function properties of miRNAs add robustness to gene-regulatory networks making the exploration and regulation of miRNAs extremely therapeutically exciting.

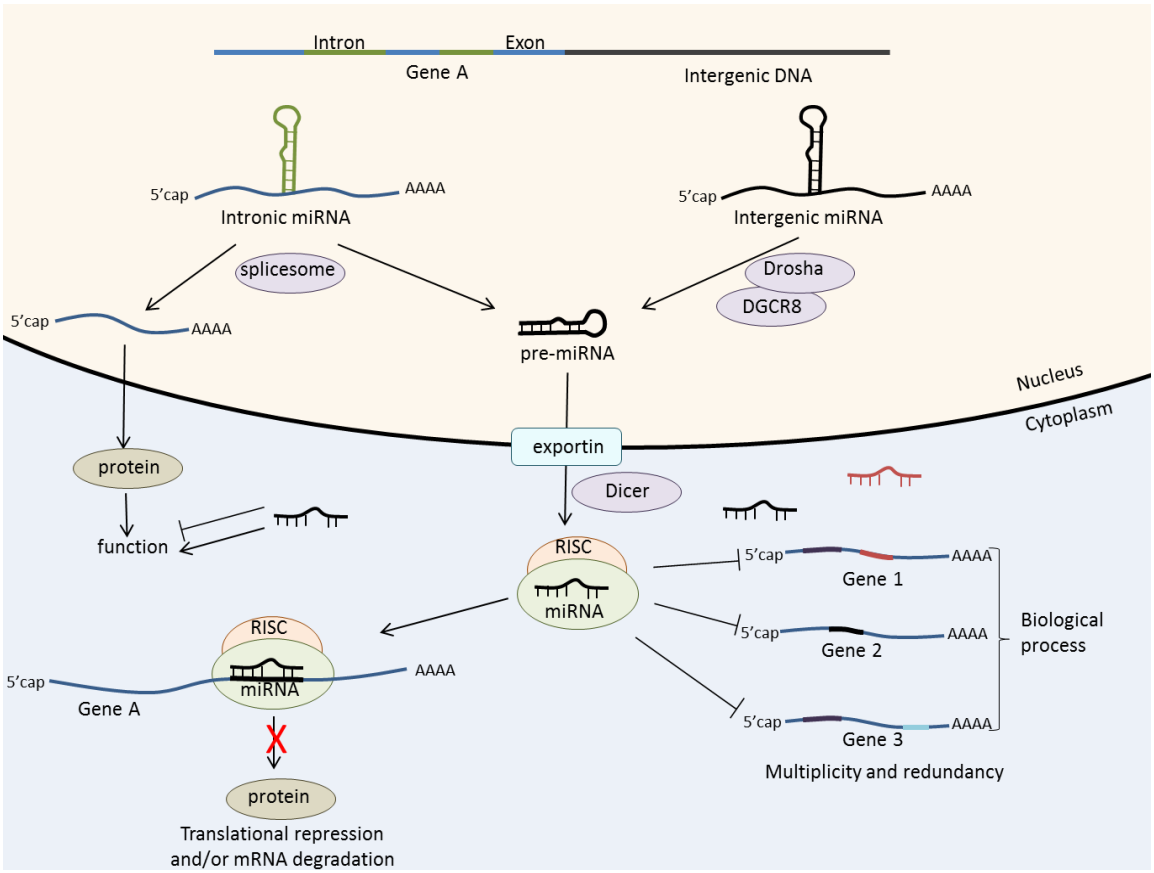

Figure 3.1. miRNA biogenesis and functional concepts. From the introns of pre-mRNA or the non-coding regions of the genome, miRNAs are transcribed as long precursors which are cleaved by Drosha and DGCR8 into pre-microRNAs and are actively transported to the cytoplasm to be further cleaved by dicer into a miRNA duplex. Subsequently, one strand of the miRNA is assembled into the RNA-induced silencing complex (RISC) to guide the sequence-specific recognition of its target mRNA leading to mRNA degradation or translational repression (gene A). Since intronic miRNAs are transcribed at the same times as its host gene it is common for the miRNA to regulate a similar process as the protein it was transcribed from. A characteristic of miRNAs is the ability of a single miRNA to regulate multiple mRNAs in a biological process (gene 1, 2 and 3). In addition, multiple miRNAs can target the same mRNA adding redundancy and cooperation between miRNAs.

1.4 miRNAs in Cardiovascular Disease

The importance of miRNAs in cardiovascular development and function was initially observed after Dicer deletion in myocardial and vascular lineages produced lethal phenotypes four days after birth.[56, 57] The dynamic regulation of numerous cardiac-enriched miRNAs during cardiac stress indicates their involvement in the regulation of cardiovascular disease.[58-63] More specifically, several studies indicate a crucial role for miRNA-dependent regulation of a number of different cellular processes following MI, such as cardiac angiogenesis, fibrosis, and cardiomyocyte hypertrophy (as reviewed in [64]) (Figure 1.2). Since miRNAs play a significant role in the regulation of CVD, an understanding of their regulation and function is pivotal for the study of disease and the development of therapeutic strategies that enhance reparative miRNAs or inhibit detrimental miRNAs to augment repair after MI. Consideration should also be given to understanding how current therapies, such as collagen matrices, regulate miRNAs, as it may provide important mechanistic insight towards their optimization.

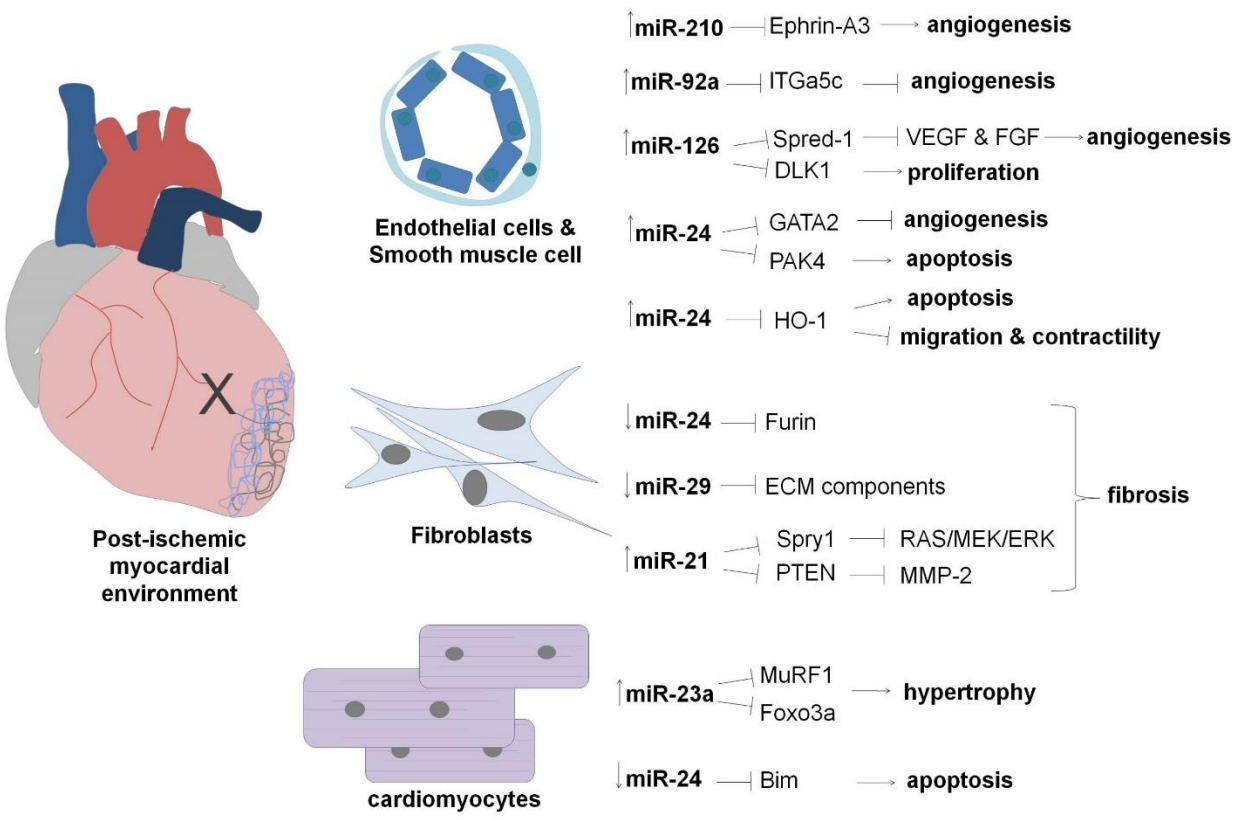

Figure 1.2. miRNA regulation and function in the ischemic/infarcted myocardium. Targets of key miRNAs and the processes they regulate in myocardial ischemia/infarction are shown.

1.4.1 miRNA-21

To date, the role of miR-21 in cardiovascular disease can be described as controversial. Thum *et al*. observed a robust up-regulation of miR-21 in cardiac fibroblasts in a mouse model of cardiac failure.[65] Within the fibroblasts, sprouty homologue 1 (Spry1) was identified as a direct target of miR-21; and Spry1 is a potent inhibitor of the Ras/MAPK/ERK pathway that regulates fibroblast survival and growth factor secretion.[65-67] *In vivo* silencing with antimiR-21 in a mouse pressure-overload-induced cardiac hypertrophy model reduced cardiac ERK–MAPK activity, inhibited interstitial fibrosis and attenuated cardiac dysfunction, thus highlighting the therapeutic

potential of targeting miR-21.[65] In a model of ischemia/reperfusion (IR) injury, it was demonstrated by *in situ* hybridization (ISH) that miR-21 up-regulation in the mouse heart occurred at 2 and 7 days after injury and was found to be localized specifically within fibroblasts of the infarct zone.[44] It was also shown that miR-21 regulates matrix metalloprotease-2 (MMP-2) expression in cardiac fibroblasts via a phosphatase and tensin homologue (PTEN) pathway, thus identifying another miR-21 mechanism.[44] Another study using lateral LV wall samples from patients with severe aortic stenosis (AS) undergoing aortic valve replacement therapy showed higher myocardial expression levels of primary transcripts as well as mature miR-21 in comparison to a group of surgical controls with no pressure or volume overload and normal left ventricular mass.[68] ISH using digoxigenin-double-labelled specific miR-21 probes showed that the signal in AS patient samples was restricted to cells in the interstitial space, presumably fibroblasts, with only a very week hybridization signal in the LV myocardium of the control patients, thus reinforcing the specific localization and up-regulation of miR-21 in fibroblasts.[68] In contrast, Patrick *et al*. demonstrated that miR-21-null mice and LNA-antimiR-21 treated mice displayed cardiac hypertrophy, fibrosis and loss of cardiac contractility similar to wild-type littermates after various cardiac stresses, indicating that miR-21 does not play an important role in pathological cardiac remodelling.[69] The opposing evidence for the involvement of miR-21 in cardiac disease could be, in part, due to a compensatory mechanism activated in the persistent absence of miR-21, which may be different from pharmacological inhibition of a miRNA in an adult organism. Another factor could be attributed to the differences in chemistry and oligonucleotide length of the short LNA-modified antimiR-21 and longer cholesterol conjugated antagomiR, but still there is no consensus.[70-72]

1.4.2 A Role for miRNA-92a in Angiogenesis

A member of the highly conserved miR-17~92a cluster, miR-92a is expressed in human endothelial cells and plays a role in controlling the growth of new blood vessels.[73, 74] Forced over-expression of miR-92a in human endothelial cells blocks sprout formation, inhibits vascular network formation and reduces cell migration and adhesion.[74] Similarly, systemic administration of miR-92a targeting antagomiRs delivered at 0, 2, 4, 7 and 9 days after MI increased the number of blood vessels, improved cardiac function and reduced infarct size in mice.[74] ISH with 3`-DIG labeled LNA probes performed on 2-day post-MI cardiac tissue identified that miR-92a was inhibited in the endothelium and other cell types within the myocardium.[74] Catheter-based delivery of LNA-92a after ischemia/reperfusion in pigs, increased capillary density in the border zone of the infarcted hearts and increased Itgα5 expression.[75] LNA-92a treatment also reduced the number of leukocytes in the infarcted region, improved left ventricular end-diastolic pressure and conferred direct cardiomyocyte protection, demonstrating a secondary role for miR-92a independent of angiogenesis.[75]

1.4.3 A Role for miRNA-92a in Inflammation

Studies have also linked miR-92a to a role in inflammatory endothelial dysfunction, which can lead to atherosclerosis. Endothelial cells exposed to "athero-prone" low sheer stress (SS) conditions and oxidized low-density lipoproteins had increased miR-92a levels in comparison to cells exposed to "athero-protective" high SS conditions.[73] In corroboration, miR-92a was highly expressed in the aortic arch of atherogenic $Ldlr^{-/-}$ mice compared to normal animals, and *in vivo* miR-92a inhibition altered the development of atherosclerosis, decreasing plaque size and promoting a more stable lesion phenotype in $Ldlr^{-/-}$ mice.[73] It is possible that these effects are

mediated through the miR-92a enduced up-regulation of Kruppel-like factor 2 (KLF2) as the miRNA is reduced in the endothelium during atheroprotective laminar flow.[76] In addition to the atheroprotective effects of miR-92a inhibition in endothelial cells, an inflammatory role has also been established in macrophages. It was demonstrated that stimulation of the toll-like receptor (TLR) resulted in reduced miR-92a levels within macrophages, which increased mitogen-activation protein kinase kinase 4 (MMK4) levels and the production of inflammatory cytokines (TNF-α and IL-6). [77] Furthermore, it has been shown that polarisation has an effect on miR-92a levels in macrophages, with miR-92a expression significantly higher in M1 macrophages than in M2 macrophages.[78]

1.5 miRNA Regulation for Therapeutic Purposes

With the relative ease by which miRNAs can be manipulated pharmacologically, and the fact that miRNAs are involved in almost every aspect of cardiovascular health and disease, we are presented with interesting therapeutic opportunities for the treatment of MI.[79] *In vivo*, pharmacological intervention can be accomplished with the use of miRNA mimics and/or anti-miRNAs (Figure 1.3). Anti-miRNAs are modified antisense oligonucleotides harbouring the full or partial complementary reverse sequence of a mature miRNA. The application of an anti-miRNA leads to a reduction in endogenous miRNA levels. In therapy, they would be applied to activate gene expression by binding to the pathological miRNA, de-repressing the miRNAs inhibitory effects on target gene expression [79-81]. To increase cellular uptake, anti-miRNAs can be conjugated to cholesterol (termed antagomiRs) which are capable of binding to cell surface membrane receptors. Antisense oligonucleotides (ASOs) can also contain a modified sugar backbone which increases specificity and affinity to bind and inhibit miRNA function.[45] For example locked

nucleic acids (LNA) are modified RNA nucleotides with a methylene bridge connecting the 2' oxygen, and 4'carbon of the ribose backbone.[82] Systemic delivery of anti-miRNAs has proven to be sufficient for the reduction of miRNAs levels in cardiac tissue for an extended period of time.[83] In contrast, miRNA mimics are synthetic double-stranded RNA which have been modified for cellular uptake and stability. Similar to endogenous miRNAs, miRNA mimics are loaded into RISC by the cell, and function to elevate endogenous protective miRNA levels by further inhibiting target mRNA expression.[83] Despite the recent discovery of miRNAs in 1993, the therapeutic regulation of miRNAs already shows huge potential for the treatment of disease, with numerous miRNA therapeutic trials in non-human primates and clinical trials for the miR-122 ASO to treat chronic hepatitis C virus (HCV) infection currently already underway.[84] It is important to note that the use of anti-miRs and miRNA mimics to alter the abundance of a miRNA also provide necessary tools to study molecular functions, giving us better insight into the molecular mechanism of disease.

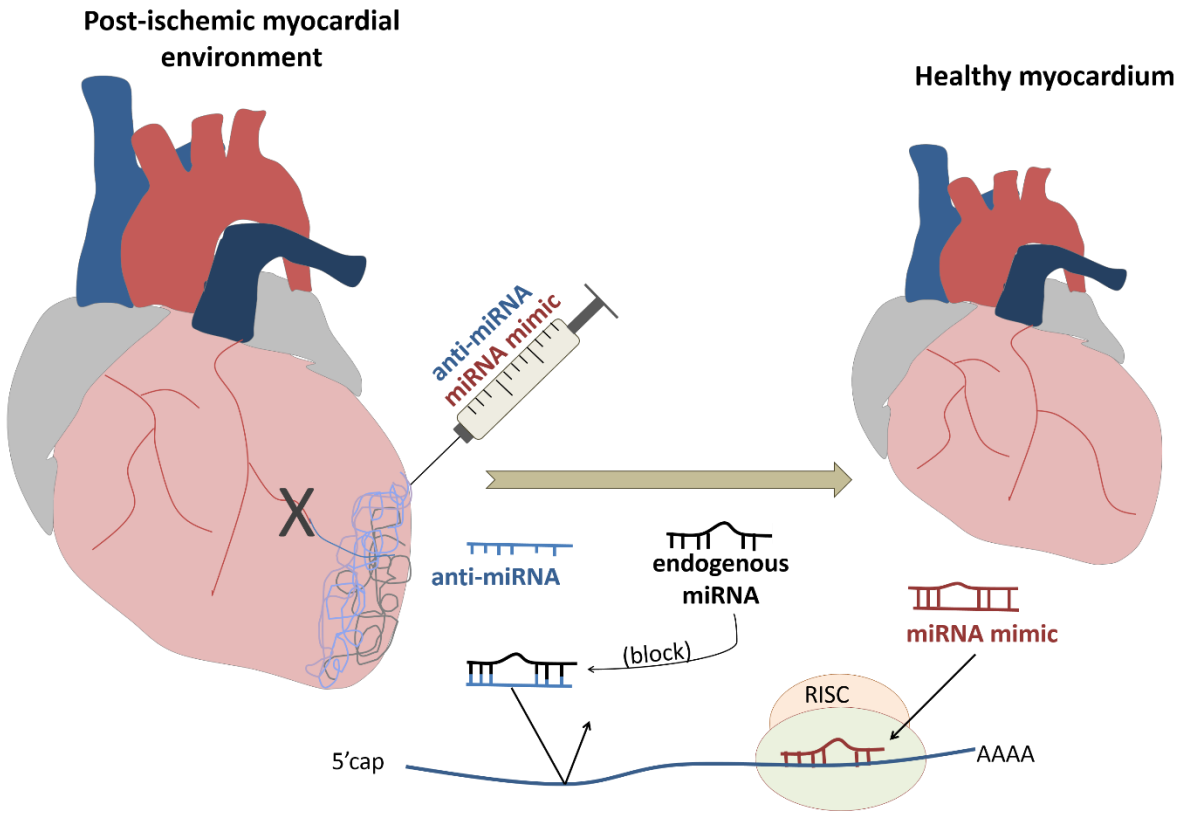

Figure 1.3. Clinical perspectives for cardiac repair using miRNA-based therapies. The ease by which miRNAs can be manipulated pharmacologically provides a therapeutic opportunity to alter miRNA levels dysregulated during ischemia/infarction to promote cardiac repair. Anti-miRNAs bind to endogenous miRNAs preventing them from binding to their target, thus increasing target gene expression. In contrast, miRNA mimics increase endogenous miRNA levels and reduce target gene expression through translational repression or mRNA degradation.

1.5.1 Challenges Associated with miRNA Regulation

Issues associated with the delivery of therapeutic RNAs begins with the challenge of the RNA exiting the circulatory system, crossing the cellular membrane in the target tissue and entering the cytoplasm. First, the removal of double stranded RNAs from the bloodstream by nucleases and phagocytic cells, such as macrophages, and the filtering and excretion of molecules less than 50kDa by the kidneys has challenged the systemic delivery of miRNA duplexes to target tissue.[85, 86] Second, complexed RNAs larger than 5nm in diameter, cannot cross the capillary endothelium and will remain in the circulatory system until excreted.[85] Encapsulation of miRNAs within a lipid vesicle to minimize excretion and enhance uptake is commonly employed to help address these issues.[85] Third, it is also important to note that therapies using miRNA mimics and anti-miRNAs, particularly with systemic administration, can lead to unwanted side effects since they can be taken up by non-target tissues. For these reasons the localised delivery of miRNA therapeutics is highly favorable. In a study using large animals,, different techniques to administer LNA-miR-92a were examined and showed that localised delivery of a higher concentration of anti-miRNA failed to induce a further reduction of miR-92 within the myocardium, but significantly increased repression within non-target tissue in comparison to the delivery of a lower dose.[75] The study also showed that systemic delivery of LNA-miR-92a did not significantly improve global myocardial function or capillary density within the border zone of infarcted hearts whereas localised delivery did.[75] This highlights the importance of minimizing therapeutic concentration and local delivery to reduce off target effects. It also shows the need to develop strategies for tissue-specific delivery of miRNA therapeutics capable of evading the immune system. Since multiple doses are usually required to sustain miRNA levels for 20 to 30 days due

to inefficient delivery or degradation, strategies to improve site-specific delivery could also diminish the amount of times the therapeutic needs to be delivered.[85]

1.5.2 Biomaterials for miRNA Regulation and Delivery

The use of biomaterials to deliver miRNA therapeutics has only recently emerged and has focused mainly on the use of nanoparticles to encapsulate miRNA therapeutics to try and protect them and enhance their delivery efficiency (as reviewed in [87]). Of interest, it was recently shown that a collagen scaffold could be used to deliver miR-29B to fibroblasts and reduce levels of its targets, collagen type I and type III.[88] The miR-29b doped matrix was also able to improve collagen type III/I ratios when applied to a wound.[88] It has also been shown that nano-bioglass ceramic particles up-regulate miR-30c in osteoblasts offering a potential mechanistic explanation for the materials ability to cause cellular differentiation.[89]

1.6 Research Plan

1.6.1 Rationale

MI results in cardiomyocyte death, inflammation and adverse cardiac remodeling leading to the deterioration of cardiac function. It has been shown that an injectable collagen-based matrix delivered at 3-hours post-MI ameliorates the infarct environment by altering macrophage polarization, reducing cell death, enhancing angiogenesis, and reducing infarct size, resulting in improved cardiac function (unpublished, N. Blackburn). The biomaterial shows promise as a therapeutic; however, the mechanisms underlining these effects remain unclear. miRNAs, which can regulate multiple genes within a biological process, are likely involved in mediating the effects of matrix treatment Understanding these mechanisms will help in the optimization of cardiac biomaterial therapies. Furthermore, biomaterials have the potential to effectively deliver miRNA-

based therapies. The ability to control endogenous miRNA expression and concomitantly deliver miRNA therapeutics makes collagen matrix therapy attractive for treating MI.

1.6.2 Aims and Objectives

1) Identify miRNA(s) regulated by the biomaterial in a mouse model of MI and their mechanism(s) of action using a combination of *in vivo* and *in vitro* models.
2) Explore the biomaterial's ability to deliver functional miRNAs *in vitro.*

1.6.3 Hypothesis

We hypothesize that miRNA contribute to the beneficial effects of matrix treatment in the infarcted myocardium. In addition, we believe that the therapeutic effects of matrix therapy may be enhanced by using the matrix to locally deliver miRNA mimics and/or antagomirs that further augment or activate additional beneficial reparative processes.

METHODS AND MATERIALS

2. Materials and Methods

2.1 Part A: Endogenous miRNA Regulation in Matrix Therapy for MI

Animal Model and Surgical Procedure

All animal work was performed with the approval of the Animal Care Committee at the University of Ottawa Heart Institute. C57BL/6J mice (female, 7-9 weeks old; Charles River, Sherbrooke, Canada) were anesthetized and underwent a permanent left anterior descending (LAD) coronary ligation to induce myocardial infarction (MI), as previously described.[33] [ref] Briefly, the mice were intramuscularly injected with 0.1ml of buprenorphine 1 hour before the surgery for pain reduction. Prior to the surgery, the mice were sedated with 2%-3% isoflurane and 2% oxygen nasally and the chest was depilated with hair removal cream. The mice were then intubated with a 20G catheter (BD Biosciences) that was connected to an air pump set at 200uL of air and 150 strokes /minute. An incision in the chest was made and the ribs were split to expose the heart. Using a 6.0 silk suture (Syneture), the LAD was ligated with one stitch, and additional stitches were added if the blanching of the heart was not severe enough. After the ligation, the ribs and the skin were closed with #5 synthetic thread (Syneture). Three hours post-MI the mice were randomly assigned to receive 4-5 intramyocardial injections (50uL total) of: i) no treatment (SHAM), ii) PBS injections or iii) collagen matrix injections using a 27G ¼ needle (BD Biosciences) into the infarct tissue. The injections were guided by echocardiogram, while the mice were sedated with 2% isoflurane anaesthetic. The mice were sacrificed two days after treatment delivery, the cardiac tissue was perfused with heparin-PBS and the infarct and peri-infarct area was dissected, snap frozen and stored at -80°C. RNA isolations were performed on the tissue for microRNA microarray analysis (3 mice/treatment group) and microarray validation by RT-qPCR

(5 mice/ PBS and matrix treatment group). PBS- and matrix-treated mice (5mice/group) were also generated for protein work.

Matrix Preparation

The collagen matrix was prepared on ice in a chilled round bottom glass centrifuge tube, as previously described.[90ref] Briefly, 1ml of type 1 rat tail collagen (4.41mg/ml; BD Biosciences) and 200µl of a cross-linking solution containing 0.1M 2(-N-morpholino) ethanesulfonic acid (MES) buffer (pH~6.0) and a 1:1 molar ratio of 1-Ethyl-3-(3-dimethylaminopropyl)carbodiimide (EDC) and N-hydroxysuccinimide (NHS) was added to the tube and mixed thoroughly. PBS (400µl) and 100µl of 20% chondroitin sulfate-C in $Ca2^{+}$/$Mg2^{+}$ free PBS (Wako, Osaka, Japan) was also added to the mixture. Lastly, the pH was adjusted to 7.2±0.2 using 1N NaOH. The matrix was then loaded into a 27G ¼ needle and syringe for the myocardial injections or plated into a 6-well plate (180µl/well) or 12-well plate (100µl/well). The plates were placed at 37°C for 1 hour to allow the matrix to solidify. After gelation the matrices were washed three times with PBS for 5min to remove excess cross-linking reagent prior to use in subsequent experimentation.

RNA Isolation

Prior to starting RNA work the lab space and equipment was cleaned with RNase Away (Thermo Scientific) to remove RNase contamination. For isolating RNA from the cardiac tissue, 200µl of TRIzol (Life Technologies) was added to the snap frozen tissue with one scoop of 2.0mm zirconium silicate beads (Ideal Scientific) in a 1.5ml Eppendorf tube. The tubes were placed in a bullet blender (Integrated Science Solutions) at 4°C for 5min intervals at speed 8 until the tissue was fully homogenized. The supernatant was transferred to a new 1.5ml Eppendorf tube and the

volume was made up to 1ml with TRIzol. 200µl of chloroform was added to the samples, which were then shaken vigorously by hand for 15s and incubated at room temperature (RT) for 10min. The samples were spun at 12,000×g for 15min at 4°C. The top phase containing the RNA was transferred to a new tube and 500µl of isopropanol was added, mixed by inversion and incubated for 10min at RT to precipitate the RNA. The samples were then spun at 12,000×g for 10min at 4ºC and the pellet was washed with 75% Ethanol (EtOH). The samples were spun at 7,500×g for 5min at 4ºC and the pellet was re-suspended in 50µl of Ultra Pure distilled water (Invitrogen). RNA from all *in vitro* samples was isolated using the miRNeasy Micro Kit (Qiagen). Briefly, the media was aspirated off the cells, the cells were washed twice with PBS and lysed with 1ml of QIAzol Lysis Reagent (Qiagen). The lysate was incubated at RT for 5min and transferred to an Eppendorf tube. A 200µl volume of chloroform was added and the samples were spun at 12,000×g for 15min at 4ºC to allow phase separation. The upper phase containing the RNA was extracted and a 1.5× volume of 100% EtOH was added to precipitate the RNA. The RNA was cleaned on a column to produce high-quality RNA. All RNA samples were stored at -80°C.

RNA Quality and Integrity

The NanoDrop-1000 Spectrophotometer with V3.3 Software (Thermo Scientific) was used to analyse RNA concentration and quality. Briefly, the machine was blanked with 1µl of Ultra Pure distilled water before loading 1µl of sample. The sample concentration was given in ng/µl and used to normalize the amount of RNA that was reverse transcribed into cDNA. The 260/280 ratio was checked, which measures the purity (protein or phenol contamination) of nucleic acids and should be ~2.0. The 260/230 ratio, a secondary measurement of RNA purity, was also checked to be in the range of 1.8-2.2. If these ratios were lower than expected and the RNA was isolated

without a column, then the RNeasy MinElute Cleanup Kit (QIAGEN) was utilised to remove contaminants. The user's manual was followed, except that 100% EtOH was used instead of the RPE buffer and 80% EtOH to ensure the retention of small RNAs (i.e. miRNAs) on the column during the washing steps. The Agilent RNA 6000 Nano Kit (Agilent Technologies) and the 2100 Bioanalyzer instrument with the 2100 Expert Software (Agilent Technologies) were used to analyse the integrity of the RNA. Briefly, 1µl of denatured RNA samples at a concentration between 25-500ng/µl were loaded onto the RNA chip with the gel-dye mix, RNA marker and Ladder. The chip was vortexed on the IKA vortex mixer at 2,400rpm for 1min before being placed in the Bioanalyzer, which separates the RNA based on size. The RNA integrity number (RIN) was then utilized to estimate the integrity of the total RNA with a RIN of 10 indicating no degradation and a RIN of 1 indicating a completely degraded sample. A RIN of 7 of higher was used as a minimum threshold for microarray RNA.

miRNA Microarray

RNA samples from the infarct and peri-infarct area of 3 SHAM mice, 3 matrix-treated mice and 3 PBS-treated mice were processed for miRNA microarray analysis. A 500ng sample of RNA for each mouse was labelled with the FlashTag Biotin HSR RNA Labeling Kit (Affymetrix). Briefly, poly (A) tailing of the total RNA was performed followed by ligation of the biotin-labelled 3DNA molecule to the RNA. The samples were then stored at -20°C until profiling. The samples were brought to the StemCore microarray facility for miRNA microarray profiling on Affymetrix GeneChip miRNA Arrays, which use Streptavidin-PE for Biotin detection.

Statistical Interpretation of miRNA Profile and miRNA Target Prediction

Statistical interpretation of the miRNA microarray was performed by Alphonse Chu (Marjorie Brand lab, OHRI). Online miRNA target gene prediction programs were used to find predicted miRNA targets for the top miRNA candidates identified with the microarray. The gene prediction sites that were used were TargetScan, miRDB and miRanda. The miRSystems database which integrates seven well-known miRNA target prediction programs was also used to identify promising miRNA targets and pathways regulated by the miRNA. Finally, the location of the mature miRNA in the genome was searched using miRBase. 10 miRNAs with targets whose functions match the observed functional benefits in matrix-treated MI hearts were selected for further analysis.

Reverse Transcription and qPCR for miRNA Expression Analysis

Primers for miR-21 and the 10 promising miRNA candidates identified by the miRNA microarray, as well as a housekeeping gene, were ordered from QIAGEN. The following miScript Primer Assays were ordered: miR-21 (MS00009079), miR-433-5p (MS00006279), miR-296-5p (MS00016436), miR-3572-3p (MS00042749), miR-382 (MS00032809), miR-466a-5p (MS00022015), miR-375 (MS00032774), miR-763 (MS00003087), miR-377 (MS00002275), miR-92 (MS00005971) and RNU6B (MS00014000). Total RNA, including miRNA, was reverse transcribed to cDNA using the miScript II RT kit (QIAGEN). Briefly, 4µl of 5x miScript HiSpec Buffer, 2µl of 10x miScript nucleics Mix, 2µl miScript Reverse Transcriptase Mix, template RNA (10ng - 2µg) and Ultra Pure distilled water were added to a 0.5ml Eppendorf tube for a total volume of 20µl. The sample was gently mixed and centrifuged before being placed in the Mastercycler Gradient (Eppendorf). The Mastercycler settings were set to 37°C for 60min followed by 95°C for

5min. The samples were diluted 1 in 5 with water and stored at -20°C until eventual use. For qPCR, a master mix for the housekeeping gene and every miRNA of interest was prepared. The volume per reaction for each of the reagents was: 10µl of 2x QuantiTect SYBR green PCR Master Mix, 2µl of miScript Primer Assay, 2µl of 10x miScript Universal Primer and 4µl of Ultra Pure distilled water. A total of 6µl of cDNA for each target being analyzed was pipetted into a 0.5ml Eppendorf tube. The master mix for each target was added to the tubes containing the cDNA; 20µl of the solution was pipetted into a white 96-well LightCycler 480 Multiwell Plate (Roche) in triplicates. The plate was sealed with LightCycler 480 Sealing Foil (Roche) and vortexed for 1min in the Mini Plate Spinner-MPS 1000 (Labnet). The plate was then placed in the LightCycler 480 Real-Time PCR System (Roche). The cycling conditions were 15min at 95°C for the initial activation step and 40 cycles of denaturation for 15s at 94°C, annealing for 30s at 55°C and extension for 30s at 70°C, followed by a melting curve step. After the run, the melting curves for each target were analyzed to ensure single product formation. Relative quantification was used for the gene of interest by normalizing to the RNU6B housekeeping gene.

Reverse Transcription and qPCR for miRNA Target Genes

The following mouse-specific primer sequences were ordered to assess the gene expression of miR-21 and miR-92a targets in the cardiac tissue, fibroblasts and BMDMs: m-Spry1-F (ATGGATTCCCCAAGTCAGCAT), m-Spry1-R (CCTGTCATAGTCTAACCTCTGCC), m-S1P1-F (ATGGTGTCCACTAFCATCCC), m-S1P1-R (CGATGTTCAACTTGCCTGTGTAG), M-Rap1b-F (ATGCGTGAATATAAGCTCGTCG), m-Rap1b-R (GCGAAGCCTTGTCCGTTCT), m-ItgA5-F (CTCCCTCTACAACGTCTCAGG), M-Iga5-R (CATCRCCATTGGTATCAGTGGC), m-ItgaV-F (TTGATTCAACAGGCAATCGAGA), m-

ItgaV-R (AGCATACTCAACGGTCTTTGTG), m-18S-F (GTAACCCGTTGAACCCCATT) and m-18S-R (CCATCCAATCGGTAGTAGCG). RNA was reverse transcribed to cDNA using the IScript Reverse Transcription Supermix for RT-qPCR (BIO RAD). Briefly, 4µl of 5x iScript reverse transcription supermix, template RNA (1pg - 1µg) and Ultra Pure distilled water were added to a 0.5ml Eppendorf tube for a total volume of 20µl. The sample was gently mixed and centrifuged before being placed in the Mastercycler Gradient (Eppendorf). The Mastercycler settings were set to 25°C for 5min followed by 42°C for 30min and 85°C for 10min. The samples were diluted 1 in 10 with water and stored at -20ºC until further use. For qPCR, a master mix for every gene of interest was prepared. The volumes of the reagents per reaction were: 10µl of SsoAdvanced SYBR Green Supermix (BIO RAD), 0.4µl of 10µM forward and reverse primer and 7.2µl of Ultra Pure distilled water. A total of 6µl of cDNA for each target being analyzed was pipetted into a 0.5ml Eppendorf tube. The master mix for each target was added to the tubes containing the cDNA. A 20µl volume of the solution was pipetted into a white 96 well LightCycler 480 Multiwell Plate (Roche) in triplicates. The plates were sealed with LighCycler 480 Sealing Foil (Roche) and vortexed for 1min in the Mini Plate Spinner-MPS 1000 (Labnet). The plate was then placed in the LightCycler 480 Real-Time PCR System (Roche). The cycling conditions were 30s at 95°C for the initial activation step and 40 cycles of denaturation for 5s at 95°C and annealing/extension for 15s at 60°C followed by a melting curve step. After the run, the melting curves for each target were analyzed to ensure single product formation. Relative quantification was used for the gene of interest by normalizing to the 18S housekeeping gene. The following human-specific primer sequences were ordered to assess the gene expression of miR-92a targets in human coronary artery endothelial cells (HCAECs) and CACs: h-S1P1-F (TTCCACCGACCCATGTACTAT), h-S1P1-R (GCGAGGAGACTGAACACGG), h-Rap1b-F

(AGCAAGACAATGGAACAACTGT), h-Rap1b-R (TGCCGCACTAGGTCATAAAAG), h-Itga5-F (GCCTGTGGAGTACAAGTCCTT), h-Itga5-R (AATTCGGGTGAAGTTATCTGTGG), h-ItgaV-F (ATCTGTGAGGTGGAACAGGA), h-ItgaV-R (TGGAGCATACTCAACAGTCTTTG). RT-qPCR was performed as described above.

TaqMan Gene Assays

cDNA prepared with the IScript Reverse Transcription Supermix for RT-qPCR was thawed on ice, gently vortexed and briefly spun. A master mix for every sample and gene of interest was prepared in a 1.5ml Eppendorf tube and contained 1µl of 20× TaqMan Gene Expression Assay, 10µl of 2× TaqMan Universal Master Mix II, no UNG (Applied Biosystems), 4µl of cDNA (1-100ng) and 5µl of RNAse-free water. The Gene Expression Assays used were human Itgα5 (Applied Biosystems, Assay ID Hs01547673_m1), human ItgαV (Applied Biosystems, Assay ID Hs00233808_m1) and human 18S (Applied Biosystems, Assay ID Hs99999901_s1). The tubes were inverted, briefly centrifuged and 20µl of the solution was pipetted into a white 96-well LightCycler 480 Multiwell Plate (Roche) in triplicates. The plates were sealed with LightCycler 480 Sealing Foil (Roche) and vortexed for 1min in the Mini Plate Spinner-MPS 1000 (Labnet). The plate was then placed in the LightCycler 480 Real-Time PCR System (Roche). The cycling conditions were 10min at 95°C for the initial activation step and 40 cycles of 95°C for 15s and 60°C for 1min. Relative quantification was used for the gene of interest normalized to a housekeeping gene (18S).

Circulating Angiogenic Cell Isolation and Cell Culture

Procedures for the isolation of human CACs were approved by the Human Research Ethics Board of the University of Ottawa Heart Institute. Twelve tubes of blood (~10cc per tube) was collected with a 21G needle into EDTA vacutainer tubes from each healthy human volunteer and layered onto 20ml of Histopaque 1077 (Sigma-Aldrich). Density-gradient centrifugation at 2160rpm for 30min was performed to separate the different blood components. The buffy coat, containing the peripheral blood mononuclear cells (PBMCs), was isolated with a disposable plastic pipette into a falcon tube. The cells were washed two times with wash buffer (0.833ml of 6.5% EDTA, 0.5ml of FBS diluted to 50ml with PBS) and spun for 10 minutes at 1400rpm. The cells were re-suspended in Endothelial Basal Media-2 (Clonetics) that was supplemented with EGM-2-MV SingleQuot Kit Suppl. & Growth Factors (Clonetics) containing 5% fetal bovine serum, 50ng/ml human VEGF, 50ng/ml human insulin-like growth factor-1, 50ng/ml human epidermal growth factor and antibiotics. The cells were then plated onto four 10cm plates, coated with fibronectin from human plasma (Sigma Aldrich). After four days of culture, the adherent population was lifted using PBS and a cell scraper. The cells were counted with a TC10 Automated Cell Counter (BioRad) using counting slides (BioRad). For all *in vitro* experiments, the cells were plated at 1.0×10^6 cells/well in a 6-well plate.

Human Coronary Artery Endothelial Cells

One vial of primary Human Coronary Artery Endothelial Cells (HCAECs; purchased from ATCC) was thawed and plated at 5,000 cells per cm^2. The cells were cultured in Vascular Cell Basal Medium (ATCC) that was supplemented with P/S and the Endothelial Cell Growth Kit-VEGF (ATCC) for a final concentration of 5ng/ml of rh VEGF, 5ng/ml of rh EGF, 5ng/ml of rh

FGF basic, 15ng/ml rh IGF-1, 50µag/ml of ascorbic acid, 10mM of L-glutamine, 0.75 Units/ml of heparin sulfate, 1µg/ml of hydrocortisone hemisuccinate and 2% FBS. Once the cells reached 80% confluence they were lifted using 0.5% trypsin-EDTA (Gibco) and spun at 150g for 5min. The pellet was re-suspended in media and the cells were counted with a TC10 Automated Cell Counter (BioRad) using counting slides (BioRad). For all *in vitro* experiments, the cells were plated at 5.0 x 10^5 cells/well in a 6-well plate.

Fibroblast Isolation and Culture

C57/BL6 wild-type mice were euthanized by CO_2 inhalation and cervical dislocation. The heart was perfused with heparin-PBS, excised from the chest and placed in a falcon tube containing HBSS on ice. The hearts were then finely minced using a pair of scissors and placed in dissociation buffer which contained collagenase type B and trypsin. The tissue was then rocked at 37°C for 45 min to dissociate the cells from the tissue. After 45min, the cells were filtered through a 70µm nylon cell strainer (BD Falcon) to remove any undigested tissue. Fibroblast media composed of DMEM /F12 (1:1) (Gibco) with 10% FBS and penicillin/streptomycin (P/S) was added to the cells. The cells were then spun at 1400rpm for 10min in a centrifuge. The supernatant was discarded and the pellet was re-suspended in 10 ml of media. The cell suspension was transferred to a 10cm plate and incubated at 37ºC for 120min. After 120min, the non-adherent cells were removed and discarded. Fresh media was placed on the adherent cells, containing the fibroblast population and cultured to passage 2 before being used for experiments. To lift the cells, 0.25% trypsin EDTA (Invitrogen) was added and incubated at 37ºC for 5min or until the cells were no longer adhered to the plate. The lifted cells were then transferred to a falcon tube and spun at 1400rpm for 5min. The pellet was re-suspended in media and the cells were counted with a TC10 Automated Cell

Counter (BioRad) using counting slides (BioRad). For all *in vitro* experiments, the cells were plated at 2.5 x 10^5cells/well in a 6-well plate.

Bone Marrow-derived Isolation and Culture

C57BL/6J wild type mice were euthanized by CO_2 inhalation and cervical dislocation. The legs were then removed above the hip socket with a large pair of scissors within a cell culture hood. The fur was peeled off the legs and the muscle was cleaned off of the bone using a pair of scissors. Once the tibia and femur were exposed the tibia was removed by cutting above the ankle joint and under the knee cap. A 25G needle and 20ml syringe containing PBS was inserted into the diaphysis of the tibia and used to flush the bone marrow into a falcon tube containing high glucose DMEM (Gibco). The femur was then removed by cutting under the hip joint and above the knee cap and the bone marrow was flushed using the same technique. Once the bone marrow from the desired number of legs had been isolated, the cells were centrifuged at 1,300rpm for 10min. The cell pellet was re-suspended in high glucose DMEM with 10% FBS, 15% L929 conditioned media and P/S. The cells were plated in 15cm plates (1 leg/plate) with 35ml of media and cultured for 7 days to produce bone marrow-derived macrophages. Media was changed at day 3 or 4 and every 2-3 days afterwards. To lift the cells, the media was removed and 5ml of 50mM EDTA/HBSS (without Ca or Mg) was added and placed at 4°. After 20min, the cells were scraped with a cell scraper and transferred into a falcon tube. The cells were spun at 1,300rpm for 5 min and the pellet was re-suspended in media. The cells were counted with a TC10 Automated Cell Counter (BioRad) using counting slides (BioRad). For all *in vitro* experiments, the cells were plated at 1.2 x 10^6 cells/ well in a 6-well plate.

Protein Isolation and Western Blots

All protein work was performed on ice to minimize protein degradation. For *in vitro* work, the media was aspirated off the cells, the cells were washed twice with PBS and lysed with 150ul of RIPA (20mM Tris-HCl pH 8.0, 150mM NaCl, 0.1% SDS, 1% Deoxycholic Acid, 1% Triton X-100 and 1 tablet of cocktail inhibitor (Roche) and water). Cells were lysed on ice for 20min before being transferred to a 0.5ml Eppendorf tube and spun at top speed for 15min at 4ºC. The supernatant, which contained the protein, was transferred to a 0.5ml Eppendorf tube and stored at -20ºC until further use. A protein assay was performed to determine protein concentration. Briefly, 10µl of BSA standard at 2000, 1000, 500, 250, 125, 62.5 and 31.25 µg/ml were pipetted into a 96-well microplate (Evergreen Scientific) in duplicate along with 10µl of PBS which served as a blank; 8µl of PBS and 2µl of protein was then also pipetted into the plate in duplicate. A 150µl volume of Pierce 660nm Protein Assay Reagent (Thermo Scientific) was added to all the wells, and the microplate was placed in the Synergy Max Plate Reader (BioTek) and read at 660nm. The volume necessary to add 25µg of protein was calculated based on these concentrations. Protein samples containing 25µg of protein, 5× sample buffer and PBS were prepared. Samples were boiled at 95°C for 5min and loaded onto a 10 or 15 well 1.5mm 8% sodium dodecyl sulfate-polyacrylamide gel electrophoresis (SDS-PAGE) gel with 5µl of Precision Plus Protein Standard (Bio Rad) to identify the approximate weight of the target protein. The running gel portion of the SDS-PAGE gel was prepared by mixing and pouring 8.0ml of water, 3.0ml of 40% acrylamide, 3.8ml of 1.5M Tris buffer (pH 8.8), 0.15ml of 10% sodium dodecyl sulfate (SDS), 0.15ml of ammonium persulfate (APS) and .012ml of tetramethyethylenediamine (TEMED) into a gel plate to 1cm below the base of the comb. Isopropanol was added on top and the gel was left to solidify for 45min. The isopropanol was then removed and the stacking gel was poured on top of the

running gel and left to solidify with a comb for 45min. The stacking gel was prepared with 7.5ml of water, 1.0ml of 40% acrylamide, 1.25ml of 1.0M Tris buffer (pH 6.8), 0.1ml of 10% SDS, 0.1ml of APS, and 0.010ml of TEMED. Once the gel was loaded, it was run at 120V for 90 min with running buffer. The running buffer contained 25mM Tris base, 192mM glycine and 3.5mM SDS with double distilled water. The gel was then transferred onto a methanol activated PVDF membrane for 120 min at 80V using transfer buffer. The transfer buffer contained 100ml of 10× transfer buffer (25mM Tris Base and 192mM Glycine), 200ml of MeOH and 700ml of ddH_20. The blots were blocked with 5% skim milk diluted with 0.1% TBS-T composed of 100ml 10× TBS (50mM Tris Base and 150mM NaCl with water, pH 7.4), 900ml ddH2O and 1ml Tween-20 (BioRad) for 1 hour at RT. The blots were probed overnight at 4°C with primary antibody in 5% skim milk. The primary antibodies used were: Integrin α5 (Santa Cruz, sc-10729) at a 1:500 dilution, Integrin αV (Santa Cruz, sc-376146) at a 1:500, EDG1 (Santa Cruz) at 1:5000 dilution and HSP90 (Santa Cruz, sc-13119) at a 1:1000 dilution. The blots were washed 3 times with TBST for 5min before being probed with a secondary antibody for 1 hour. The secondary antibody was prepared with 0.1% Casein, 0.1% SDS, PBS, 1:1000 dilution of IRDye700 conjugated anti-mouse IgG (Rockland) and a 1/1000 dilution of IRDye800 conjugated anti-rabbit IgG (Rockland). The blots were re-washed 3 times with TBST for 5min and scanned on the Odyssey scanner (LI-COR) with the Odyssey Version 3.0 Software. Fiji was utilized to quantify the protein bands. To standardize the amount of protein loaded onto the gel, the quantity of each protein sample was normalized to the quantity of the housekeeping gene in the sample.

2.2 Part B: Therapeutic miRNA Delivery

Preparation of Collagen Matrix Containing microRNAs for RT-qPCR Analysis

Stocks of miScript miRNA mimic Syn-cel-miR-39-3p (Qiagen, MSY0000010), miRDIAN mimic human has-miR-33a-5p (Dharmacon, C-300509-07), and miRDIAN microRNA Negative Control #1 (Dharmacon, CN-001000-01-05) were prepared at 20µM concentrations. Stocks of the miRDIAN Hairpin Inhibitor Mouse mmu-miR-33-5p (Dharmacon, IH-310581-08) and the miRDIAN microRNA Hairpin Inhibitor Negative Control #1 (Dharmacon, IN-001005-01-05) were also prepared at 20µM concentrations. An aliquot of the matrix, prepared as previously described, was added to a chilled Eppendorf tube. The miRNAs or mimics were then mixed separately into the matrix at final concentrations of 10nM, 100nM, 1000nM or 2500nM depending on the experiment. A volume of 100µl or 180µl of the miRNA-loaded matrix mixture was coated onto 6- or 12-well plates, respectively and allowed to gel for 1hour at 37ºC. The solidified matrix was washed 3 times with PBS for 5 minutes before plating cells on the matrix. Unmodified matrix was also coated onto the plate and served as an experimental control.

Cell Culture and RT-PCR with miRNA-loaded Matrix

Fibroblasts were plated at 3.0×10^5 cells/well on the 12-well plate alone, on the matrix alone and on the matrix containing 10nM or 100nM of miScript miRNA mimic Syn-cel-miR-39-3p. After 36h of culture, the cells were lifted using 0.25% trypsin EDTA (Invitrogen) for 5min and washed off the matrix into a 15ml falcon tube with PBS. The trypsin incubation and PBS washes were also performed on wells containing the matrix with mimic but no cells. This was done to determine if the mimics may wash out of the gel during the cell lifting process. Plates containing the matrices were wrapped in paraffin and stored at -80°C. The falcon tubes were spun at 1,400rpm

for 15min. The supernatant was removed from the samples containing cells and the pellet was re-suspended in 1ml of QIAzol Lysis Reagent. For the controls that did not contain cells, all but 250µl of supernatant was removed and 750µl of TRIzol LS Reagent (Invitrogen) was added. Subsequently, RNA isolations were performed using the miRNeasy Micro Kit (QIAGEN) as previously described. Leftover mimics were also isolated from the matrix by adding 1ml of QIAzol Lysis Reagent directly to the well. The NanoDrop-1000 Spectrophotometer with V3.3 Software (Thermo Scientific) was used to analyse RNA concentration and quality and the RNA was reverse transcribed using miScript II RT kit (QIAGEN). RT-qPCR for cel-miR-39 using the Ce-miR-39 miScript Primer Assay (QIAGEN, MS00019789) was performed and normalized to U6 expression. Similarly, THP1 cells were plated on the matrix containing 100nM and 1000nM of miScript miRNA mimic Syn-cel-miR-39-3p at 5.0 x 10^5cells/well and differentiated to a macrophage phenotype with 100nM of Phorbol 12-myristate 13-acetate (PMA) (Invitrogen) for 3 days. These cells were cultured in RPNI medium 1640 (Gibco) with 10% FBS and P/S. RNA isolation and RT-qPCR was performed similarly to fibroblasts.

Standard Curve for miRNA Mimic

To determine the copy number of syn-cel-miR-39 mimic taken up by the cells, a standard curve was created. The miRNA mimic was diluted to a concentration of 10^{10} copies/µl and kidney RNA, derived from murine kidneys, was used as carrier RNA. A 20µl reverse-transcription reaction was prepared with the miScript II RT kit using 5µl of diluted miScript miRNA mimic and 50ng of carrier RNA. The mixture was incubated for 60min at 37ºC and 5min at 95ºC. Following this, 480µl of 1ng/µl kidney RNA was added to the 20µl reaction and gently mixed to yield a solution containing 10^8 copies of cDNA/µl. Serial dilutions of the solution was performed to yield

dilutions with 10^7 copies/µl, 10^6 copies/µl, 10^5 copies/µl, 10^4 copies/µl, 10^3 copies/µl and 10^2 copies/µl. Real-time PCR was subsequently performed using the Ce-miR-39 miScript Primer Assay. Results were used to plot a standard curve of Ct values against log copy number.

TaqMan miRNA Assays

TaqMan microRNA Reverse Transcription Kit (Applied Biosystems) was used to reverse transcribe the RNA samples obtained from fibroblasts cultured on cel-miR-39 mimic-loaded matrix. A master mix for the desired number of RT reactions was prepared containing 0.15µl of 100mM dNTPs mix, 1µl of 50U/µl of MultiScribe Reverse Transcriptase, 1.5µl of 10× Reverse Transcription Buffer, 0.19µl of 20U/µl RNase inhibitor and 4.16µl of Ultra Pure distilled water. In a 0.5ml tube 7µl of master mix, 5µl of RNA (1-10ng) and 3µl of 5× RT primers specific for cel-miR-39 and U6 were combined bringing the total volume to 15µl. The samples were gently mixed, briefly centrifuged and incubated on ice for 5min. The tubes were then placed in the Mastercycler Gradient (Eppendorf) for 30min at 16°C, 30min at 42°C and 5min at 85°C. The samples were then stored at -20 ºC until further use. For RT-qPCR, 1µl of 20× TaqMan Small RNA Assay, 1.33µl of RT reaction product, 10µl of 2× TaqMan Universal Master Mix II, no UNG, and 7.67µl of H_2O were pipetted into each tube. The TaqMan Small RNA Assays used were TaqMan microRNA assay cel-mir-39-3p (Applied Biosystems) and TaqMan microRNA assay U6 snRNA (Applied Biosystems). The tubes were then inverted to mix and briefly centrifuged before being loaded into a 96-well plate. The plates were sealed with LightCycler 480 Sealing Foil (Roche) and vortexed for 1min in a Mini Plate Spinner-MPS 1000 (Labnet). The plate was then placed in the LightCycler 480 Real-Time PCR System (Roche). The cycling conditions were 10min at 95°C for the initial

activation step, 40 cycles of denaturation at 95°C for 15s and then annealing/extension at 60°C for 1min. Relative quantification was used for the gene of interest normalized to a housekeeping gene (U6).

Transfection and 3'UTR Luciferase

HEK293 cells were cultured in high glucose DMEM (Gibco) with 10% FBS and seeded at 2.0×10^5 cells per well in a 12-well plate. Upon reaching ~80% confluence, the cells were transfected with an ABCA1 plasmid. Briefly, tubes containing 0.8µg of a P-EZX-MT01 plasmid (GeneCopoeia) diluted in 75µl of OptiMEM (Gibco) per well and Lipofectamine 2000 Transfection Reagent (Life Technologies) at a 3:2 Lipo:DNA ratio diluted in 75µl of OptiMEM per well were prepared. The tubes were combined and incubated at RT for 20min. After 20min, 150µl of the mix was added to the cells. After 24h of transfection, the cells were lifted by gently pipetting with PBS and plated onto the matrix alone (control) or the matrix containing 1µM of miR-33 mimic. The cells were cultured on the matrix for 48h before being lifted by gently pipetting with PBS and spun at 1,400rpm for 5min. The cells were lysed with 5× Passive Lysis Buffer (Promega) for 20min at RT on a rocker. A 3'UTR luciferase assay was performed on the lysates using the Dual-Luciferase Reporter Assay System (Promega). Briefly, 10µl of the lysates were added to a 96-well assay plate (Costar) with 20µl of LARII Reagent and read on a Glomax 96 microplate luminometer (Promega) to measure ABCA1 firefly luciferase activity. A volume of 20µl of Stop n Glo Reagent was then added to the plate and read on the plate reader to measure the renilla luciferase activity. The firefly activity was then normalized to the renilla activity and the fold change between the two conditions was calculated.

Western Blots

BMDMs were seeded at 1.2×10^6 cells per well in a 6-well plate coated with the matrix containing 1µM of miR-33 mimic or 1µM of negative control #1 for 2 days, 3 days and 5 days. Once the cell culture was complete, the matrix was digested with 1mL of 250U/ml of collagenase type I (Gibco) in HBSS for 20min at 37ºC, spun at 1,400rpm for 5 min and lysed with 150µl of RIPA. The cells were also plated on a matrix containing 2.5µM of miR-33 mimic, negative control #1, hairpin inhibitor mmu-miR-33-5p and the microRNA hairpin inhibitor negative control #1 for 3 days. For the western blots, samples were not boiled, the transfer occurred at 4ºC for 2.5h at 80V and 1:500 pAb anti-ABCA1 (Novus Biologicals) and 1:1000 HSP90 in 5% skim milk was used as the primary antibody.

T0901317 LXR Ligand

BMDMs were seeded at 1.2×10^6 cells per well in a 6-well plate coated with the matrix containing 1µM of miR-33 mimic and 1µM of negative control #1 for 2 days. After 2days of culture, T0901317, a LXR agonist, (Cayman chemical) was added to the wells to up-regulate the endogenous levels of ABCA1. After 24 hours, the experiment was stopped and a western blot was performed for ABCA1 and HSP90.

Statistical Analysis

Values are reported as mean±standard error. For western blot and qPCR analysis, data was reported as the mean fold-change of treatment to control and analyzed with either a *t*-test or a one-way ANOVA. Probability values of $P<0.05$ were considered statistically significant.

RESULTS

3. Results

3.1 Part A: Endogenous miRNA Regulation in Matrix Therapy for MI

3.1.1 The collagen matrix alters miR-21 and sprouty homologue 1 (Spry1) expression in cardiac fibroblasts

There is considerable, although controversial, evidence for the involvement of miR-21 in fibrosis post-MI, as described in chapter 1. Given that collagen matrix-treated MI mouse hearts exhibit reduced fibrosis and less adverse ventricular remodeling (Blackburn et al., unpublished data), it was hypothesized that the collagen matrix can regulate miR-21 expression in cardiac fibroblasts. To test the ability of the matrix to regulate miR-21 and one of its known targets, Spry1, cardiac fibroblasts were cultured on the matrix for three days and the expression of miR-21 and its target Spry1 was analysed. It was found that miR-21 was down-regulated by the matrix compared to standard culture on TCPS whereas the expression of one of its known targets, Spry1, was not significantly altered (Figure 3.1). This data suggests that the matrix might regulate the expression of a fibrogenic miRNA.

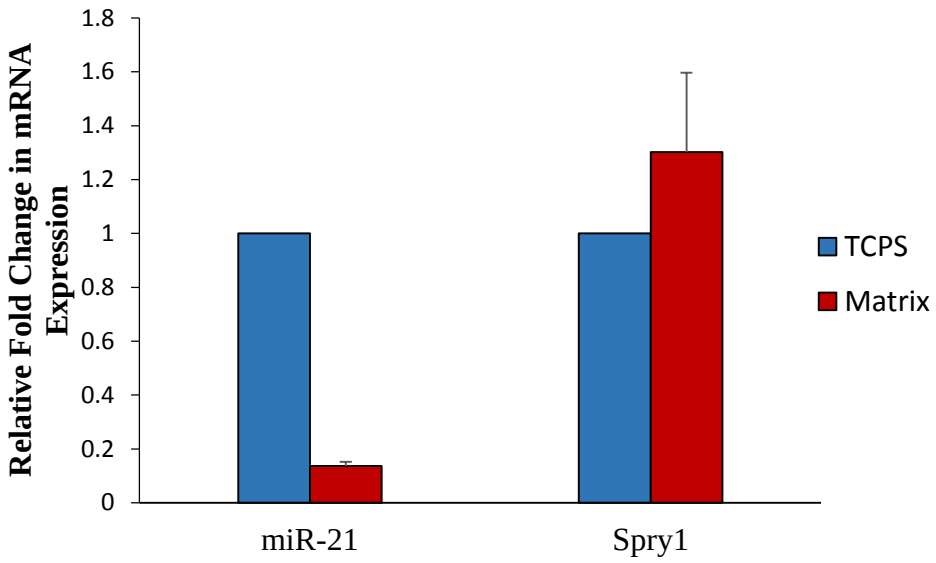

Figure 4.1. *In vitro* miR-21 expression in cardiac fibroblasts plated on the matrix and TCPS control for 3 days. MiR-21 was down-regulated in cardiac fibroblasts plated on the matrix, whereas spry1 was not significantly altered at the mRNA level. Expression was calculated as average fold change by RT-qPCR and normalized to U6 for miR-21 and HPRT for spry1 (n=2).

3.1.2 The Collagen Matrix Treatment Alters Cardiac miRNA Expression after Myocardial Infarction

A microRNA microarray on infarct and peri-infarct tissue isolated from MI mouse hearts 2 days after treatment with a collagen matrix or PBS (treatment delivered at three hours post-MI) was performed to understand how the matrix globally altered miRNA expression after MI. Cardiac tissue from SHAM mice was also profiled for comparison with a healthy heart. Of the 1966 known mature miRNA and pre-miRNA stem loops, 119 (89 mature and 30 hairpin) of them had fold changes that were greater them +/- 0.3 $\log_2$ between the matrix and PBS treatment groups as illustrated in the heat map (Figure 7.1, Appendix). Of these altered miRNAs, 69 were up-regulated with matrix treatment and 50 were down-regulated. These findings indicate that the matrix

treatment altered approximately 6% of endogenous miRNAs after MI in an upwards and downwards fashion. However, it is important to note that these differences were detected using statistics that exclude the probability of false detection.

3.1.3 Correlation of select Cardiac miRNAs Target Gene Function with Observed Benefits of Matrix Treatment

To identify potential key miRNA players involved in mediating the benefits of matrix therapy, online databases were utilized. These databases were used to identify predicted target mRNA (TargetScan, miRDB and miRanda), pathways targeted by the miRNAs (miRSystems) and the genomic location of the miRNAs (miRBase), with the hope of revealing links between the altered miRNAs and the known beneficial effects of matrix treatment post-MI. Ten miRNAs with significant fold changes between the matrix and PBS treatment groups (Figure 3.2, $0.0007 \leq p \leq 0.04$) were found to target mRNA involved in cell-matrix communication, angiogenesis, cell survival and inflammation (Table 7.1, Appendix). The ten mature miRNAs and stem-loop pre-miRNAs that were selected for future analysis were: miR-758, miR-92a-1, miR-377, miR-763, miR-375, miR-466a-5p, miR-3572, miR-296, miR-433-5p and miR-382.

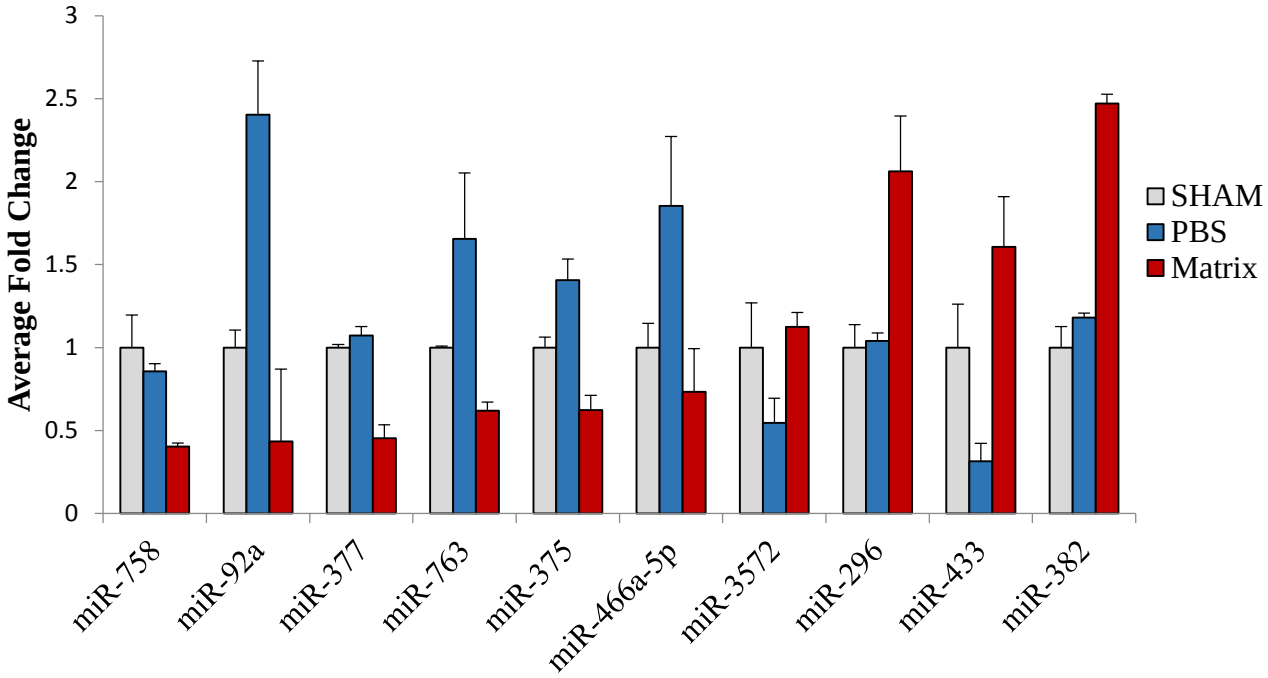

Figure 3.2 Expression profile of the ten top miRNA candidates in the infarct and peri-infarct regions 2 days after PBS and matrix treatment delivered at 3 hours post-MI. All differences between matrix and PBS treatment groups were statistically significant ($0.0007 \leq p \leq 0.04$) and were detected using the Affymetrix GeneChip miRNA Array (n=3/group).

For validating the expression of the top ten miRNAs in the matrix and PBS treated tissue, additional experimental mice for the matrix and PBS treatment groups were generated. The RNA samples from the additional (n=4-5/treatment) and the original mice used for the miRNA microarray (n=3/treatment) were cleaned using a column, reverse transcribed to cDNA using a kit able to add a poly(A) tail to miRNAs, and the expression determined by RT-qPCR using mature miRNA specific primers. The average fold change of miR-758 and miR-375 in the cardiac tissue was non-calculable due to non-congruent RT-qPCR melting curves indicating the formation of multiple products. Of the eight miRNAs that were interpretable by RT-PCR, only the mature form of miR-92a and miR-382 were significantly down-regulated by the matrix in comparison to PBS

(Figure 3.3, p=0.00047 and p=0.0372 respectively). In comparison, the mature form of miR-377, miR-763, miR-466a-5p, miR-3572, miR-296 and miR-433-5p were not significantly altered. Since miR-92a was significantly down-regulated in the miRNA microarray and RT-qPCR analysis it was selected for further analysis.

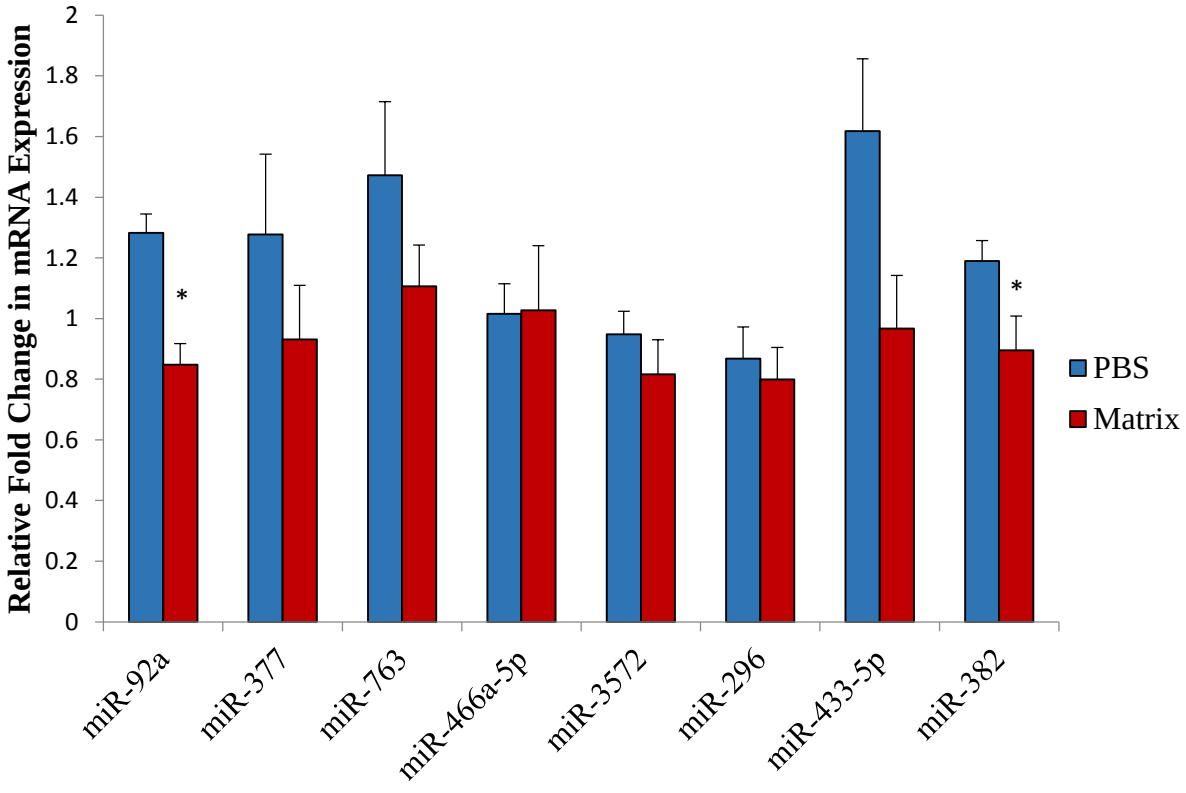

Figure 3.3. Average fold change of select miRNAs within the infarct and peri-infarct cardiac tissue 2 days after PBS and matrix treatment at 3 hours post-MI. miR-92a (*p= 0.00047) and miR-382 (*p= 0.0372) expression was significantly down-regulated in matrix-treated hearts in comparison to PBS treatment. Analysis was performed by RT-qPCR and normalized to U6; n= 8 (PBS) and n=7 (matrix).

3.1.4 Expression of miR-92a Targets in Matrix and PBS Treated Cardiac Tissue

Following the confirmation of down-regulated miR-92a expression by RT-qPCR in matrix-treated MI hearts, the expression of some of its putative mRNA targets was evaluated. Targets were identified using online miRNA target prediction databases and those with functions that correlated with the observed benefits of matrix treatment were selected for further investigation. The targets selected were integrin subunit α5 (ITGα5), integrin subunit αV (ITGαV), ras-related protein Rap-1b (Rap-1b) and Sphingosine-1-phosphate receptor 1 (S1P1) as they have all been shown to play a role in angiogenesis. RT-qPCR analysis showed that ITGaV, Rap-1b and S1P1 expression was not altered in the cardiac tissue, whereas ITGa5 was significantly down-regulated (Figure 3.4, p= 0.00488).

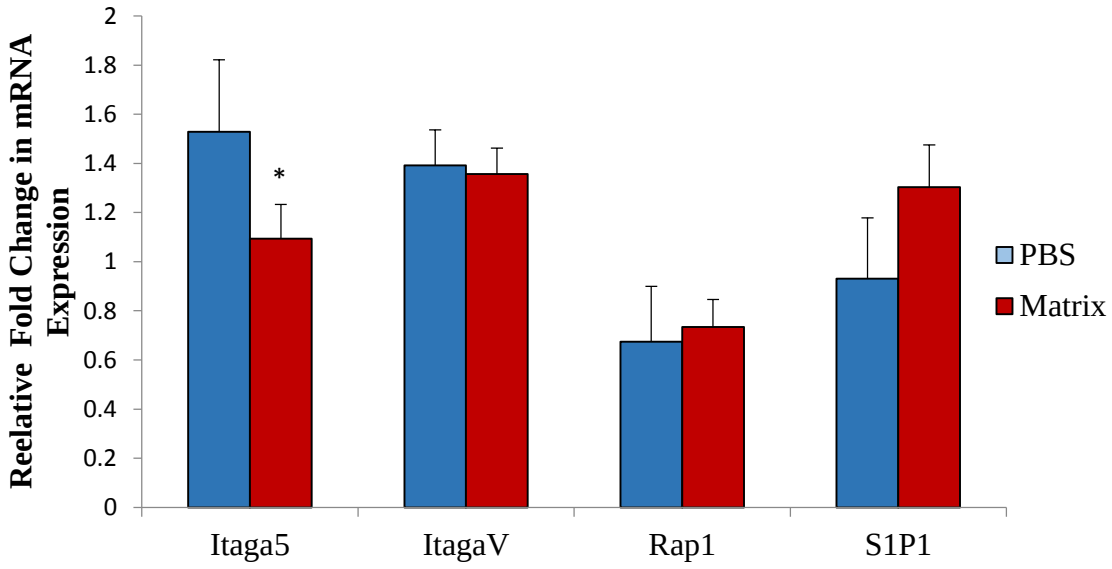

Figure 3.4. Average fold change of predicted miR-92a targets within the infarct and peri-infarct regions of cardiac tissue 2 days after PBS and matrix treatment delivered at 3 hours post-MI. ITGa5 was significant down-regulated in matrix-treated hearts 2 days after treatment (*p= 0.00488). Analysis was performed by RT-qPCR and normalized to 18S; n=8 (PBS) and n=7 (matrix).

3.1.5 Matrix Regulation of miR-92a in Circulating Angiogenic Cells

To identify the cell type(s) that may contribute to the observed down-regulation of miR-92a in cardiac tissue treated with the matrix, various cell types that are present in the infarcted heart were cultured on the matrix *in vitro* and the expression of miR-92a was examined. Two of the selected miR-92a targets, ITGa5 and ITGaV, are involved in angiogenesis and have been shown to be up-regulated in circulating angiogenic cells (CACs) that are cultured on a glutaraldehyde cross-linked collagen (porcine) matrix.[33] Therefore, these two targets were examined first. After 24 hours and 4 days of culture on the matrix in comparison to fibronectin (culture control) miR-92a levels were not significantly altered, nor were ITGa5 and ITGaV at the mRNA level, nor Itga5 at the protein level (Figure 3.5). ITGaV was not detectable at the protein level most likely due to low mRNA expression levels, as confirmed by high RT-qPCR CT values.

A

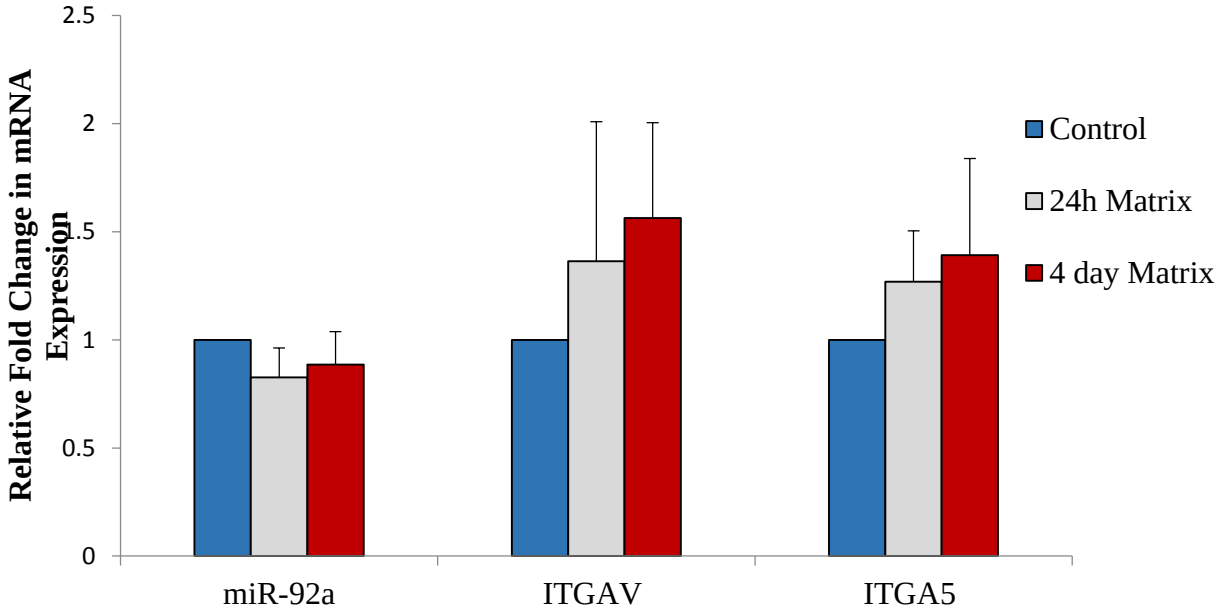
Relative Fold Change in mRNA Expression
2.5
2
1.5
1
0.5
0
miR-92a
ITGAV
ITGA5
Control
24h Matrix
4 day Matrix

B

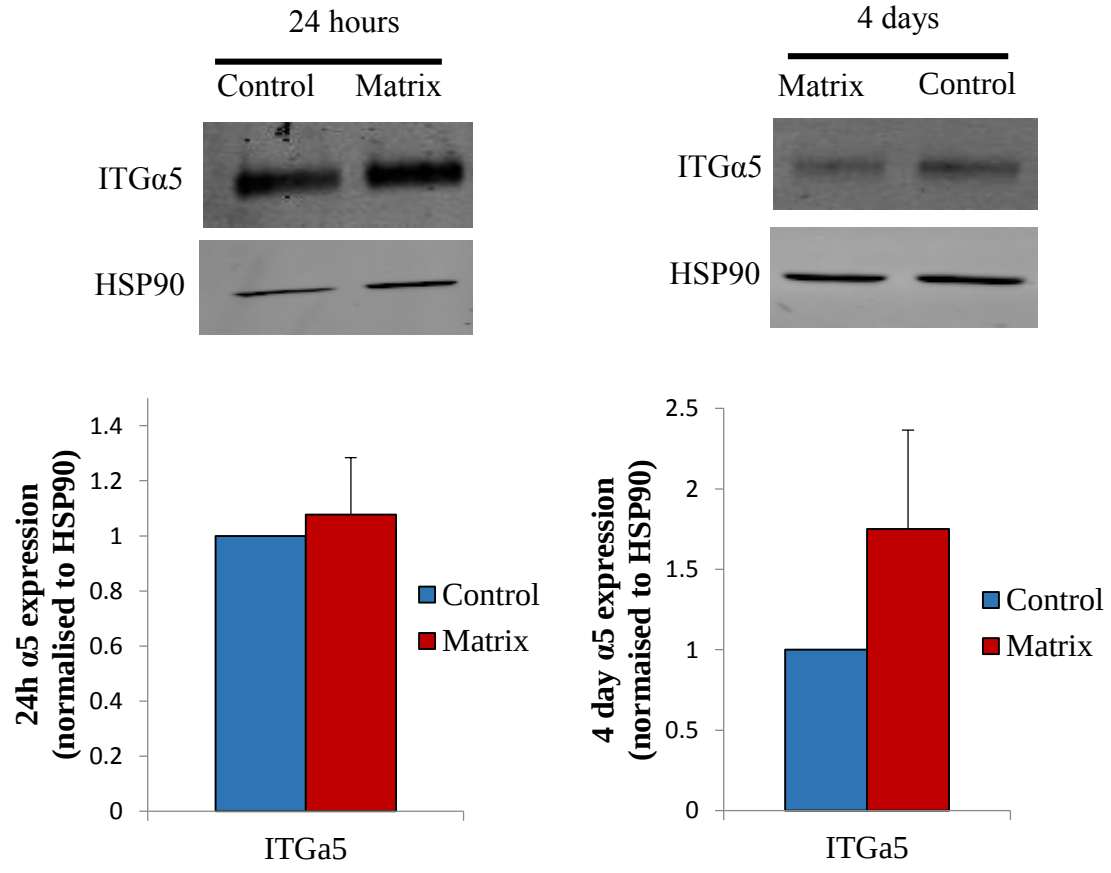
24 hours
Control
Matrix
ITGα5
HSP90
4 days
Matrix
Control
ITGα5
HSP90
24h α5 expression (normalised to HSP90)
1.4
1.2
1
0.8
0.6
0.4
0.2
0
ITGa5
Control
Matrix
4 day α5 expression (normaised to HSP90)
2.5
2
1.5
1
0.5
0
ITGa5
Control
Matrix

Figure 3.5. Expression of miR-92a, integrin α5 (ITGα5) and integrin αV (ITGαV) in circulating angiogenic cells (CACs) *in vitro*. (A) MiR-92a, ITGα5 and ITGαV expression was not significantly altered in CACs after 24h (n=4) or 4 days (n=5) of culture on the matrix. Expression was calculated as average fold change by RT-qPCR and normalised to U6 for miR-92a and 18S for ITGα5 and ITGαV. (B) Similarly, protein expression of ITGa5 was also unaltered after 24h (n=3; left panels) and 4 days (n=3; right panels). Protein levels were examined by western blot analysis and normalised to HSP90.

3.1.6 Matrix Regulation of miR-92a in Endothelial Cells

Human coronary endothelial artery cells (HCAECs) were plated on the matrix for four days and the levels of miR-92a along with ITGa5 and ITGaV were examined at the mRNA and protein level. As was observed for CACs, the matrix did not significantly alter miR-92a, ITGa5 or ITGaV levels at the mRNA and protein level (Figure 3.6). These results indicate that the matrix does not alter miR-92a levels in HCAECS *in vitro* and suggests that, despite our initial prediction, the down-regulation of miR-92a by the matrix *in vivo* may be due to the matrix interacting with a non-angiogenic cell type. Alternatively, the *in vitro* conditions may not appropriately recapitulate the post-MI environment.

A

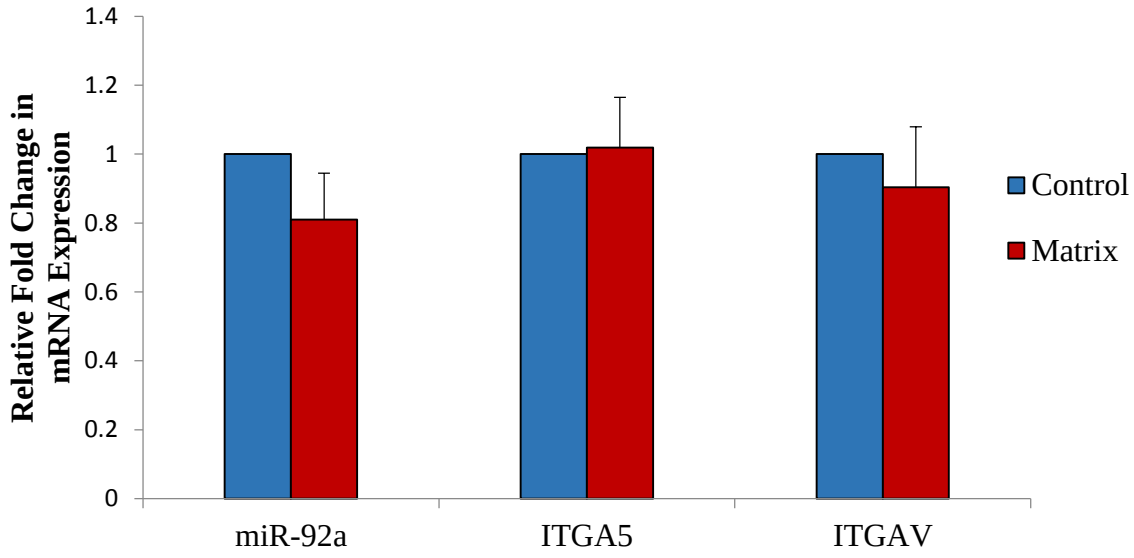
Relative Fold Change in mRNA Expression
1.4
1.2
1
0.8
0.6
0.4
0.2
0
miR-92a
ITGA5
ITGAV
Control
Matrix

B

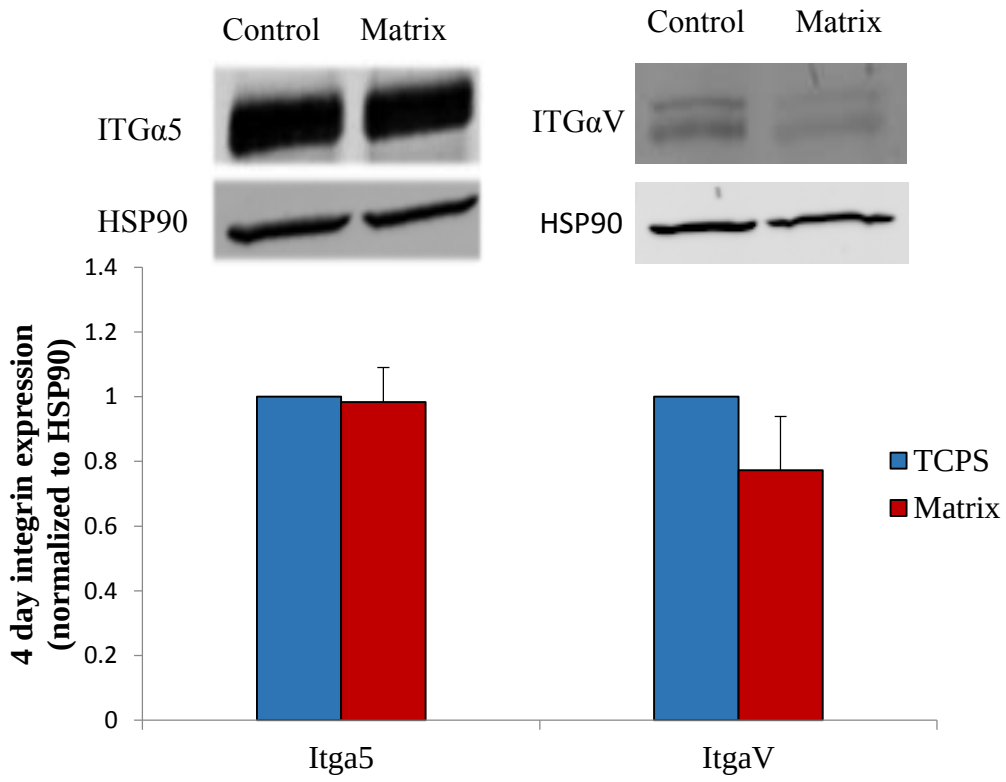
Control
Matrix
ITGα5
HSP90
Control
Matrix
ITGαV
HSP90
4 day integrin expression (normalized to HSP90)
1.4
1.2
1
0.8
0.6
0.4
0.2
0
Itga5
ItgaV
TCPS
Matrix

Figure 3.6. Expression of miR-92a, integrin α5 (ITGα5) and integrin αV (ITGαV) in human coronary artery endothelial cells (HCAECs) *in vitro*. (A) **Neither** miR-92a, nor its targets, were significantly altered in HCAECs after 4days (n=3) of culture at the mRNA level. Expression was calculated as average fold change by RT-qPCR and normalised to U6 for miR-92a and 18S for ITGα5 and ITGαV. (B) Protein expression of ITGα5 and ITGαV in HCAECs were also unaltered by the matrix after 4 days (n=3). Protein levels were examined by western blot analysis and normalised to HSP90.

3.1.7 Matrix Regulation of miR-92a in Cardiac Fibroblasts and Macrophages

Due to the fact that miR-92a levels were un-altered in angiogenic cells (HCAECs and CACs) plated on the matrix for a set number of days, other cell types involved in myocardial repair after MI were explored. First, cardiac fibroblasts were isolated from neonatal murine hearts and plated on the matrix for 24 hours. However, matrix culture did not alter miR-92a expression within this cell type *in vitro* (Figure 3.7). The regulation of miR-92a in macrophages was also explored. When bone marrow-derived macrophages were cultured on the matrix for 24 hours, a significant down-regulation of miR-92a expression was observed when compared to standard TCPS culture (Figure 3.7, p=0.0352). This data suggests that the matrix regulates endogenous miR-92a levels in macrophages *in vitro* which may explain the significant down-regulation of miR-92a observed *in vivo.*

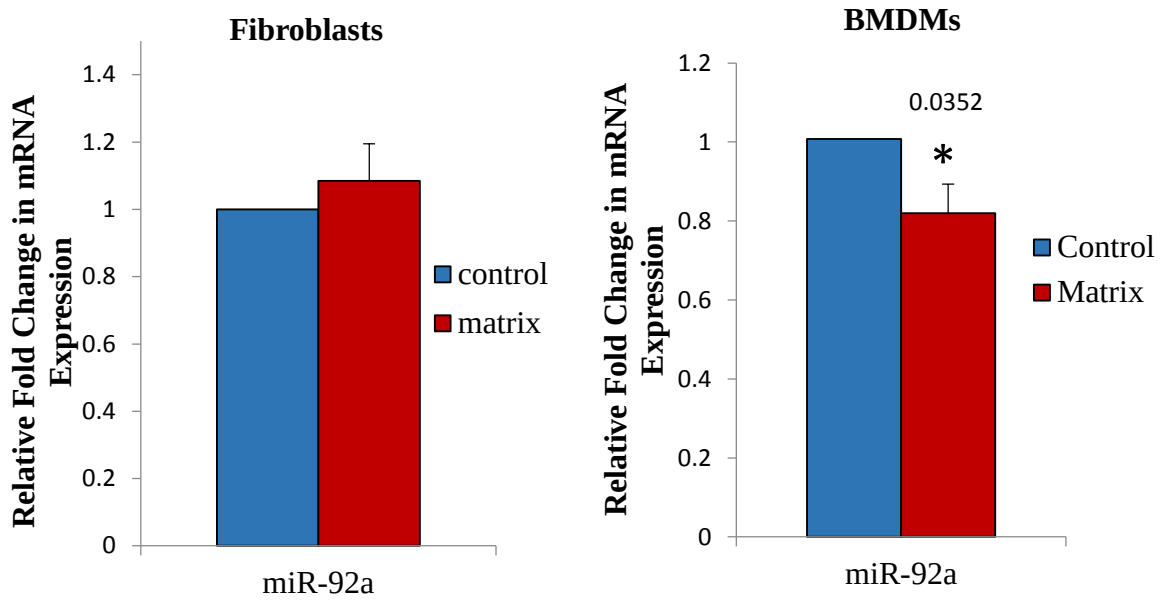

Figure 3.7. *In vitro* miR-92a expression in cardiac fibroblasts and bone marrow-derived macrophages (BMDMs). miR-92a expression was not altered in cardiac fibroblasts (n=3) but was significantly down-regulated in BMDMs plated on the matrix compared to TCPS controls (n=5, **p*=0.0352). Expression was calculated as an average fold change by RT-qPCR and normalised to U6.

3.1.8 Expression of miR-92a Targets in Bone Marrow-Derived Macrophages

The expression of the previously identified miR-92a targets were analysed in BMDM plated on a matrix vs. a TCPS control for 24 hours. No significant fold changes were observed at the mRNA level for miR-92a targets (Figure 3.8). Despite the lack of significant differences, S1P1 was up-regulated in the five samples tested and there was a trend for increased expression (*p*=0.0652). Protein levels of S1P1 in BMDMs plated on the matrix for 24 hours and 3 days were measured and found to be insignificant (Figure 3.9).

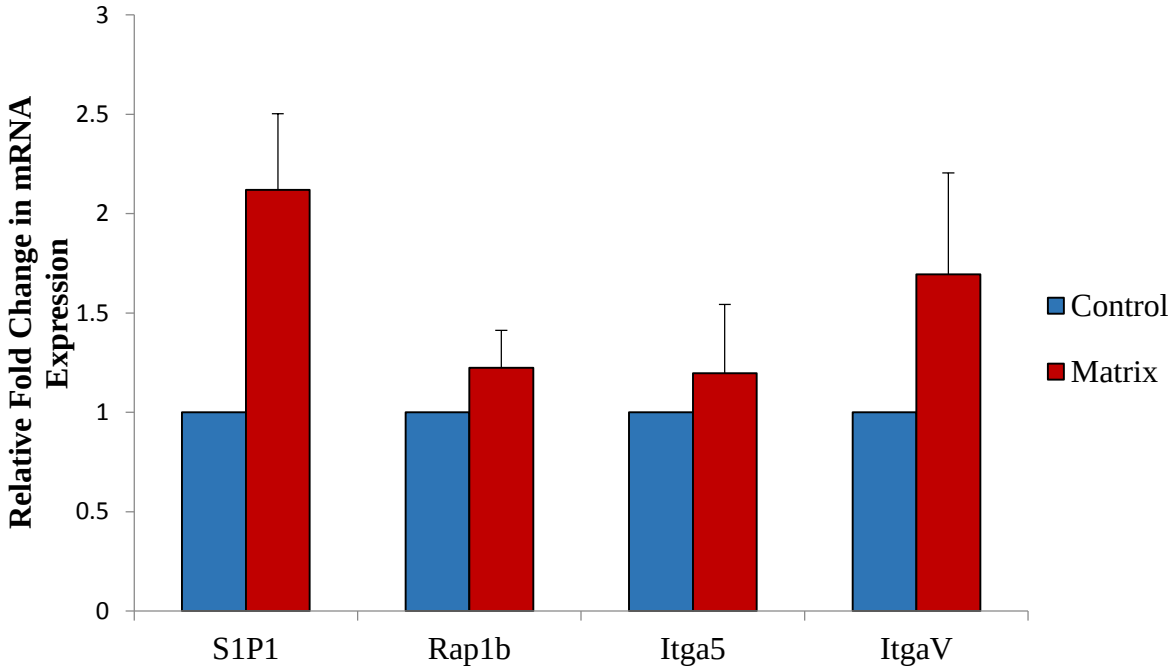

Figure 3.8. Average fold change of predicted miR-92a targets in BMDMs cultured for 24 hours. None of the mRNA targets were significantly up-regulated, although there was a trend for increased S1P1 expression (p=0.0652) in matrix-cultured BMDMs compared to those on TCPS. Analysis was performed by RT-qPCR and normalized to 18S, n=6.

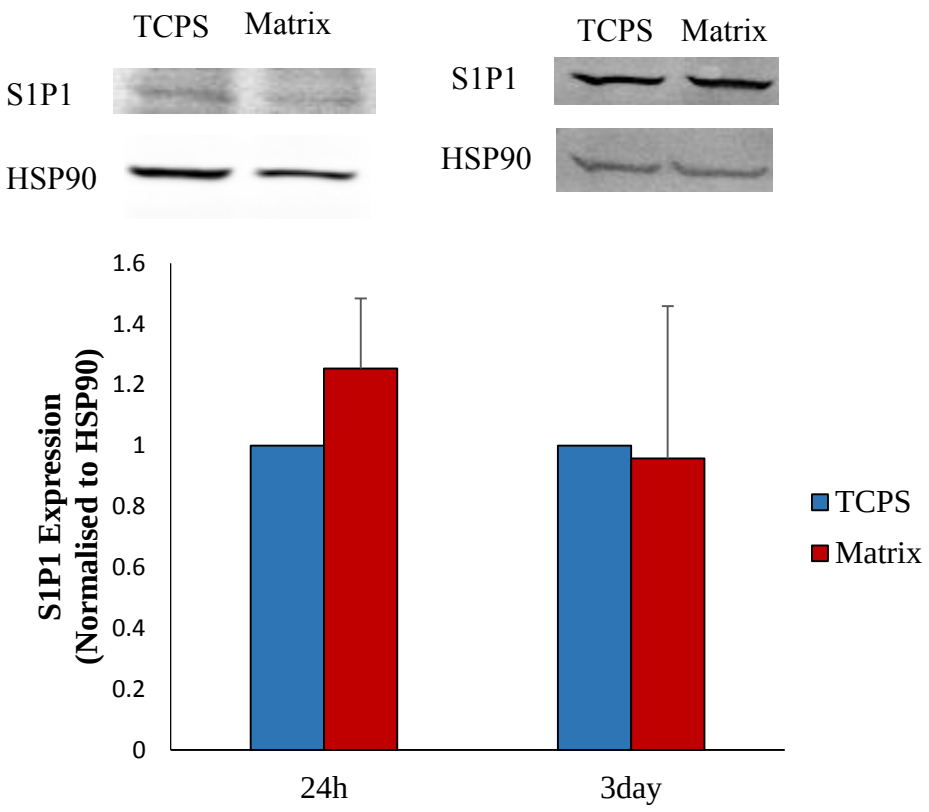

Figure 3.9. Protein level of S1P1 in BMDMs cultured for 24 hours and 3 days. Protein expression of S1P1 was unaltered in BMDMs cultured on the matrix after 24h and 3 days compared to those on TCPS (n=3). Protein levels were examined by western blot analysis and normalised to HSP90.

3.1.9 Expression of S1P1 in Matrix and PBS Treated Cardiac Tissue

Protein expression of S1P1 in the infarct and peri-infarct tissue of MI hearts treated with a matrix or PBS was examined. Five mice received LAD ligation followed by matrix or PBS treatment three hours after MI. The infarct and peri-infarct was harvested 2 days later and the protein isolated. Western blot analysis on protein showed that S1P1 was not altered in the tissue.

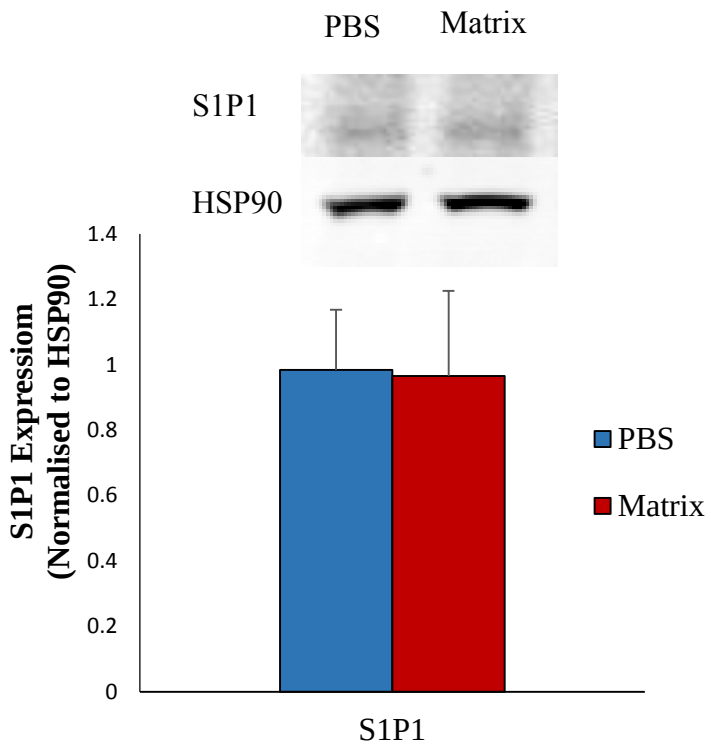

Figure 3.10. Protein level of S1P1 in infarct and peri-infarct tissue from hearts treated with the matrix or PBS delivered 3 hours after MI. Protein expression of S1P1 was unaltered by the matrix treatment in the cardiac tissue (n=5). Protein levels were examined by western blot analysis and normalised to HSP90.

3.2 Results part B: Therapeutic miRNA Delivery

3.2.1 Analyzing the Ability of the Matrix to Deliver miRNA Mimics

Cardiac fibroblasts were plated for 36 hours on a tissue culture plate, a collagen matrix and a matrix loaded with 10nM or 100nM of cel-miR-39 miRNA mimics. A miRNA mimic specific for a *caenorhabditis elegans* miRNA was utilized to ensure that the miRNAs detected in the cells by RT-qPCR originated from the matrix and were not of endogenous origin. A standard curve with the mimics was also created to calculate the copy number of mimic per sample. RT-qPCR analysis

revealed that as mimic concentration in the matrix increased, the number of mimics per sample also increased significantly (when comparing the cells & matrix to the cells & 10nM cel-miR-39 matrix and 100nM cel-miR-39 samples) indicating that the fibroblasts could be taking up the mimics from the matrix (Figure 3.11). To ensure that the possible cellular uptake was real and not a result of the mimics being washed out of the matrix, the experiment was repeated with additional controls. Matrices with 10nM and 100nM of cel-miR-39 were coated onto a plate and covered with fibroblast media for 36 hours. Trypsin-EDTA was then added to the matrix for 5min, the matrix was washed with PBS to mimic lifting cells off of the matrix and an RNA isolation was performed on the washings. RT-qPCR analysis of these samples revealed that they contained miRNA mimics levels similar to the cellular samples.

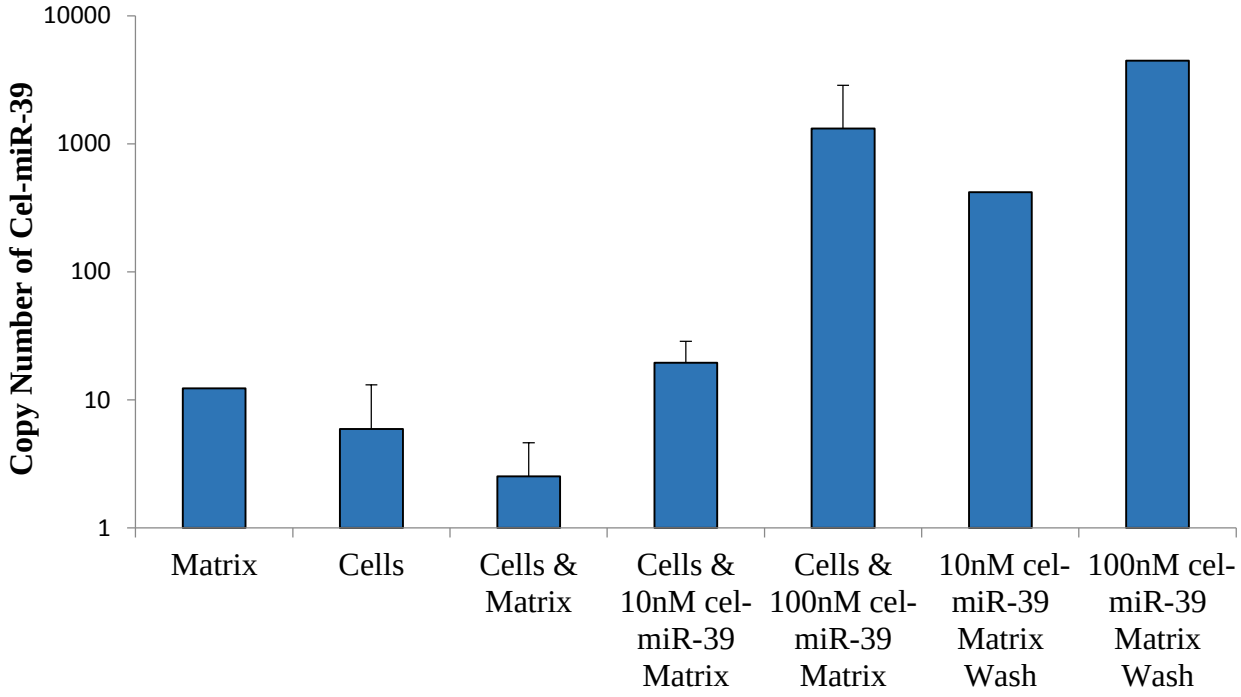

Figure 3.11. Arbitrary copies of cel-miR-39 taken up by cardiac fibroblasts from the matrix. Cel-miR-39 at concentrations of 10nM and 100nM was loaded into the matrix prior to gelation to determine the best concentration for delivery. After 36 hours of culture, fibroblasts were lifted off the matrix and analysed for cel-miR-39 uptake by RT-qPCR. Matrix alone, cells alone, cells & matrix alone were used as negative controls. Gels spiked with 10 and 100nM of cel-miR-39 were used as washing controls. n=2 for cells, cell & matrix, cells & 10nM cel-miR-39 matrix and cell & 100nM cel-miR-39 matrix, and n=1 for all other samples.

The experiment was also performed with a different cell type to ensure that the observed results were not cell-specific. Similarly, THP-1 cells were plated on the matrix but for 4 days and with 100nM and 1000nM of cel-miR-39 loaded matrices. As was observed with the fibroblast experiment, the cel-miR-39 copy number in the cells increased with increasing cel-miR-39

concentration in the matrix and was also detectable in the washing controls and samples that had never come into contact with the mimic (cells and cells & matrix) (Figure 3.12).

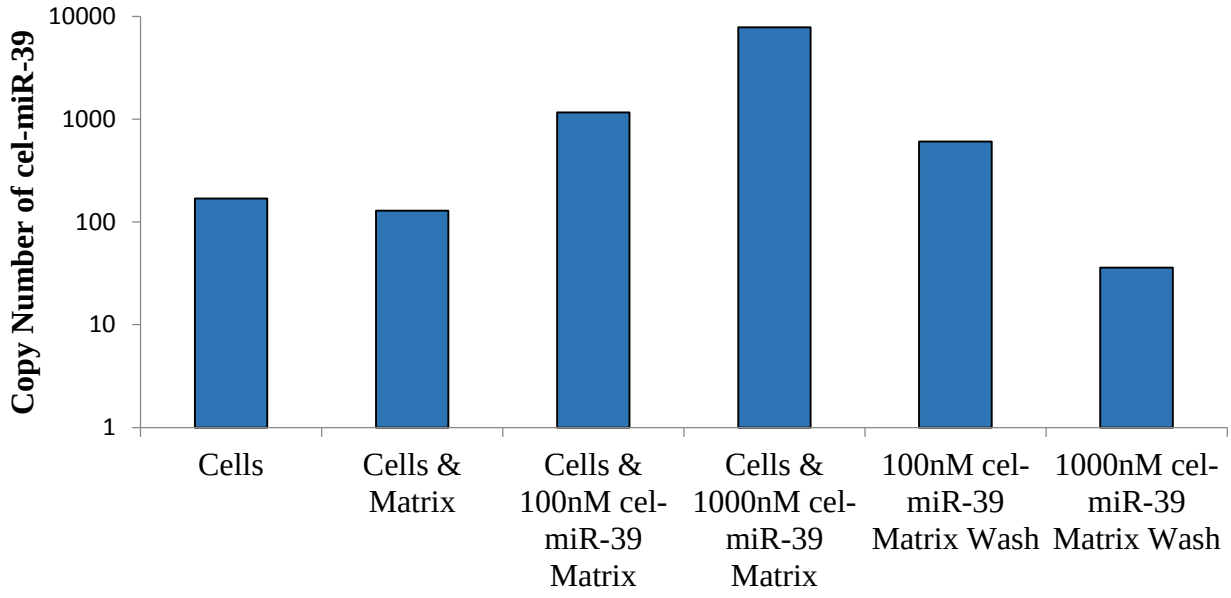

Figure 3.12. Uptake of cel-miR-39 by THP1 cells from the matrix after 4 days of culture. 100nM and 1000nM of cel-miR-39 were loaded into the matrix prior to gelation to determine the best concentration for delivery. After 4 days of culture, cells were lifted off the matrix and analyzed for cel-miR-39 uptake by RT-qPCR. Cells alone, and cells & matrix alone were used as negative controls. Gels loaded with 100nM and 1000nM of cel-miR-39 were used as washing controls. n=1 for all.

To address the false detection issues, TaqMan probes were tested on the matrix, cells, cells & matrix and cells & 100nM cel-miR-39 matrix samples from the fibroblast experiment to try and resolve the problem (Figure 3.13). The use of TaqMan probes abolished the detection of the mimic in matrix only samples. However, its detection remained in cells and cells & matrix samples

despite never having come in contact with the mimic; in fact, detection levels were similar to the cells & 100nM cel-miR-39 sample levels.

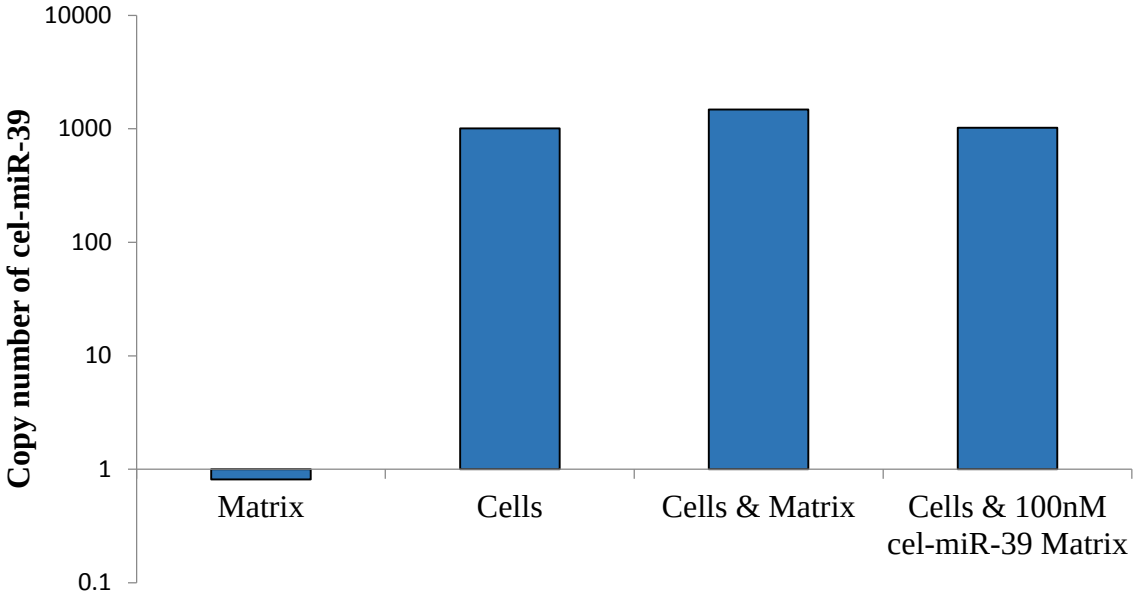

Figure 3.13. Copy number of cel-miR-39 taken up by cardiac fibroblasts after 36 hours culture on a matrix containing 100nM of cel-miR-39. RT-qPCR using TaqMan probes was performed to measure the levels of cel-miR-39. n=1 for all.

3.2.2 Analyzing the capacity of the Matrix to Retain miRNA Mimics

The capacity of the matrix to retain miRNA was also examined by quantifying the mimic copy number retained within the matrix after the delivery experiment with fibroblasts was performed. RT-qPCR demonstrated that the matrix was capable of retaining the mimics with the matrix (Figure 3.14).

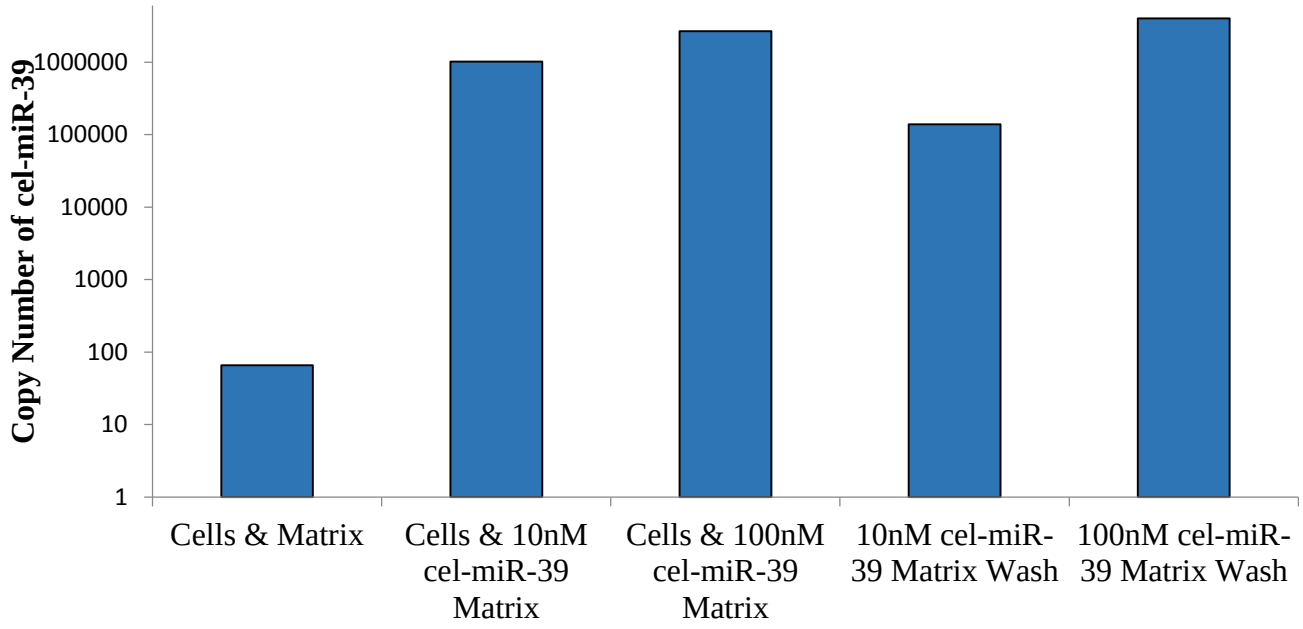

Figure 3.14. Copies of miR-39 remaining in the gel after fibroblast culture for 36 hours. cel-miR-39 copy number was determined by RT-qPCR. n=1.

3.2.3 Analysing the Ability of the Matrix to Deliver miRNA Mimics with a 3'UTR Luciferase Assay

Due to the detection of cel-miR-39 in samples that had never some in contact with the mimic, as well as its detection in the washing controls, it was difficult to deduce from the previous experiments whether or not the mimics were being taken up and/or delivered by the matrix. Therefore, a 3'UTR luciferase assay was used to detect cellular uptake. This experiment consisted of transfecting HEK293 cells with a plasmid containing the 3'UTR of ABCA1. Transfected cells were then cultured on a matrix containing 1μM of miR-33 mimic. The 3'UTR of ABCA1 was used because it is a well-characterized target of miR-33. A 20% reduction in luciferase activity for cells plated on the matrix containing the mimic in comparison to cells plated on the matrix alone was observed (Figure 3.15). This data indicated that the matrix was potentially able to deliver functional mimics to the cells. However, the cells did not fare well on the matrix (low viability)

and for this reason, the experiment was not replicable. The experiment was performed with other cell types (BMDMs, fibroblasts and HeLa cells) unsuccessfully as the cells were either unable to be efficiently transfected (BMDMs, fibroblasts) or were unable to be cultured on the matrix (HeLa cells).

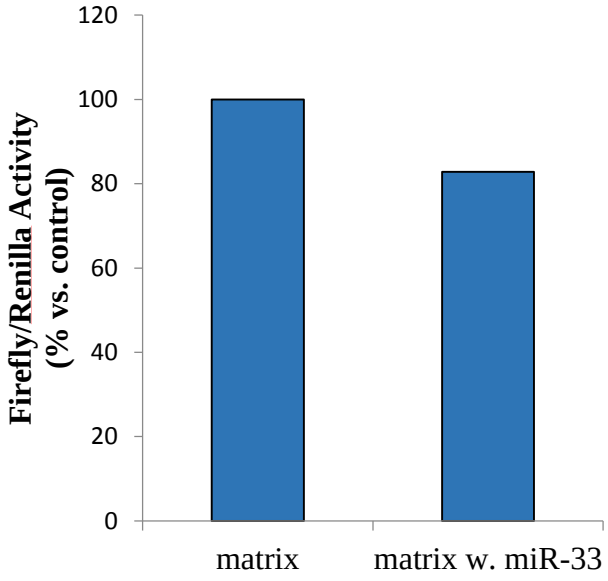

Figure 3.15. Luciferase activity in HEK293 cells transfected with a 3'UTR ABCA1 luciferase construct. After transfection, HEK293 cells were plated on the matrix or matrix containing 1μM of miR-33 mimic for 48 hours. A 20% down-regulation was observed in cells plated on the matrix containing miR-33 indicating that the matrix may be able to deliver functional miRNAs to cells. Luciferase activity was normalized to Renilla activity. n=1 for all.

3.2.4 Analyzing the Ability of the Matrix to Deliver miRNA Therapeutics by Western Blot Analysis

Due to technical difficulties with the previously utilized methods for determining cellular uptake from the matrix to cells and functionality of mimics, western blot analysis was employed. BMDMs were cultured on a matrix containing miR-33 mimics or control mimics for 2, 3 and 5

days followed by western blot analysis of ABCA1, which should be down-regulated if the mimics were properly delivered and functional. A significant down-regulation of ABCA1 was not observed in BMDMs plated on the matrix containing the mimic in comparison to the control mimic at all of the observed time points (Figure 3.16).

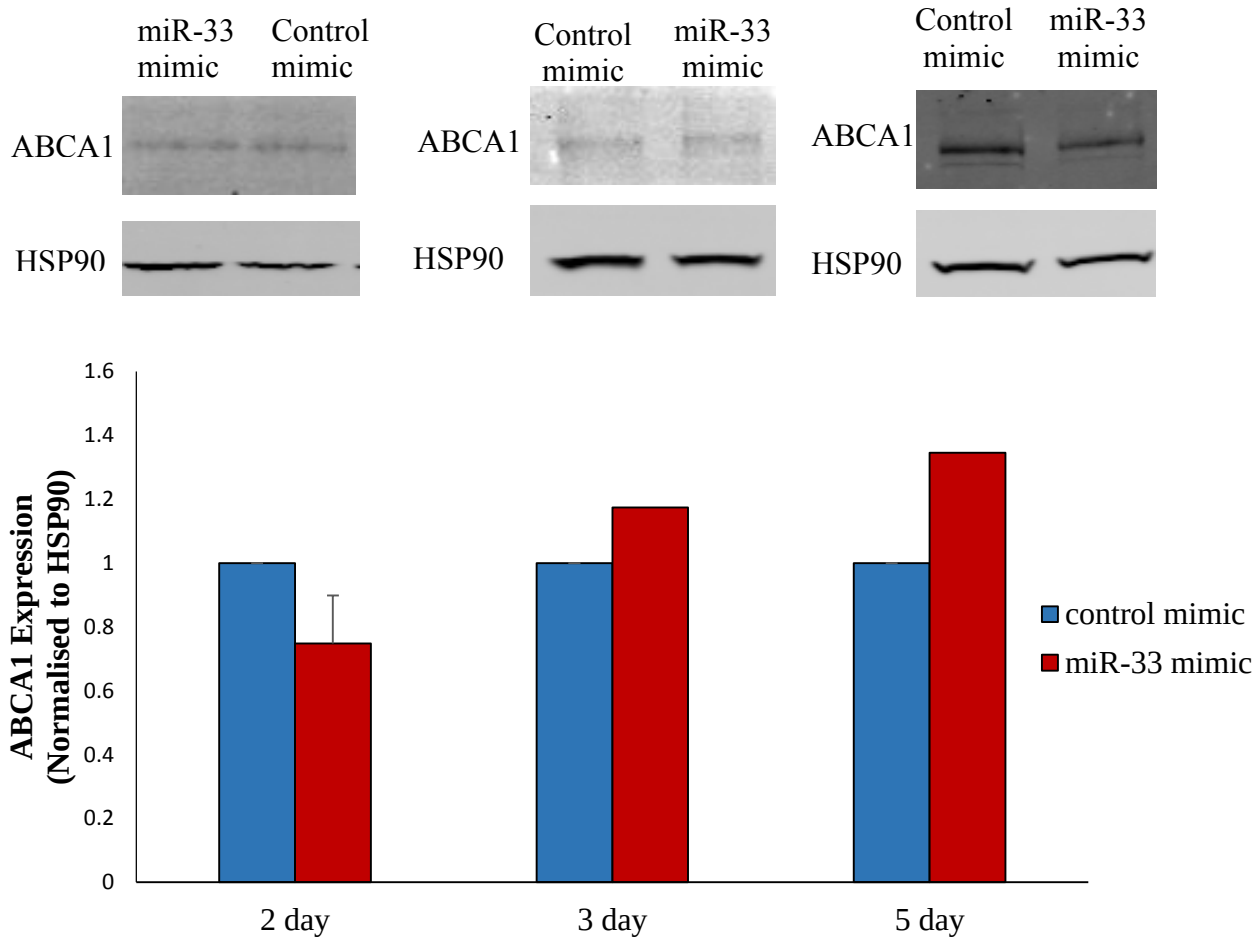

Figure 3.16. Protein expression of ABCA1 in BMDMs plated on a matrix containing 1μM of miR-33 mimic for 2 days, 3 days and 5 days in comparison to cells cultured on a matrix containing 1μM of control mimics. Protein levels were examined by western blot analysis and normalised to HSP90. The 2 day experiment was n=2 and the 3 and 5 day experiments were n=1.

A higher concentration of miR-33 mimic, as well as an anti-miR-33 (2.5µM), was then used to assess whether or not the lack of down-regulation was due to not enough mimics being taken up by the cells (Figure 3.17). No down-regulation of ABCA1 was observed in cells plated on the matrix containing miR-33 mimics, nor was an up-regulation observed in cells plated on the matrix containing the anti-miR-33 therapeutics.

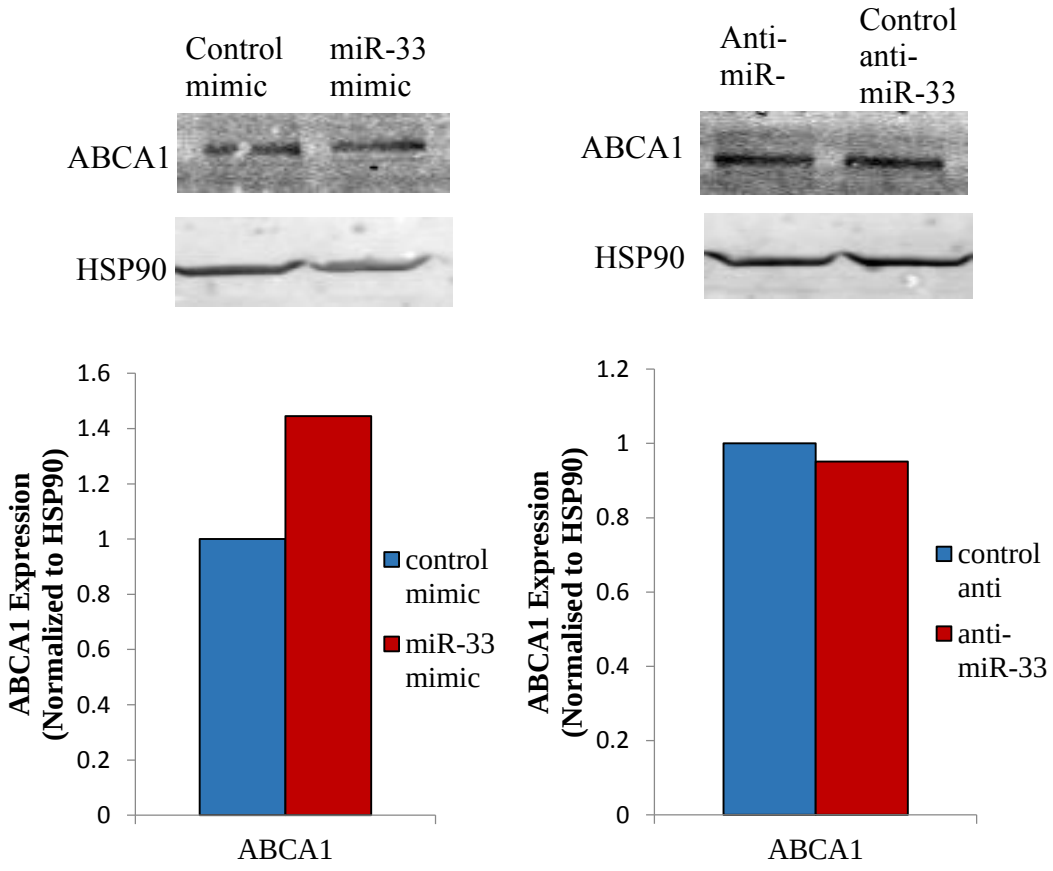

Figure 3.17. Protein expression of ABCA1 in BMDMs plated on a matrix containing 2.5µM of miR-33 mimic or anti-miR-33 for 3 days in comparison to a matrix containing 2.5µM of the appropriate control. Protein levels were examined by western blot analysis and normalized to HSP90. The experiment was n=1 and performed in duplicates.

Due to the fact that down-regulation was observed in the 3'UTR luciferase assay when the ABCA1 gene was actively being transcribed and translated (Fig. 3.15), western blot analysis was performed for BMDMs with ABCA1 up-regulation stimulated by T0901317. . T0901317 increases the expression of the ABCA1 reverse cholesterol transporter by LXR/RXR activation because it is a potent and selective LXR ligand agonist.[91] The LXR agonist was added to BMDMs plated on the matrix at day 2 of culture and a western blot for ABCA1was performed at day 3. A significant up-regulation of ABCA1 was observed between samples that had and hadn't received the agonist. However, there were no significant differences between cells plated on a matrix with the mimic vs. those plated on the matrix with the control mimic (Figure 3.18).

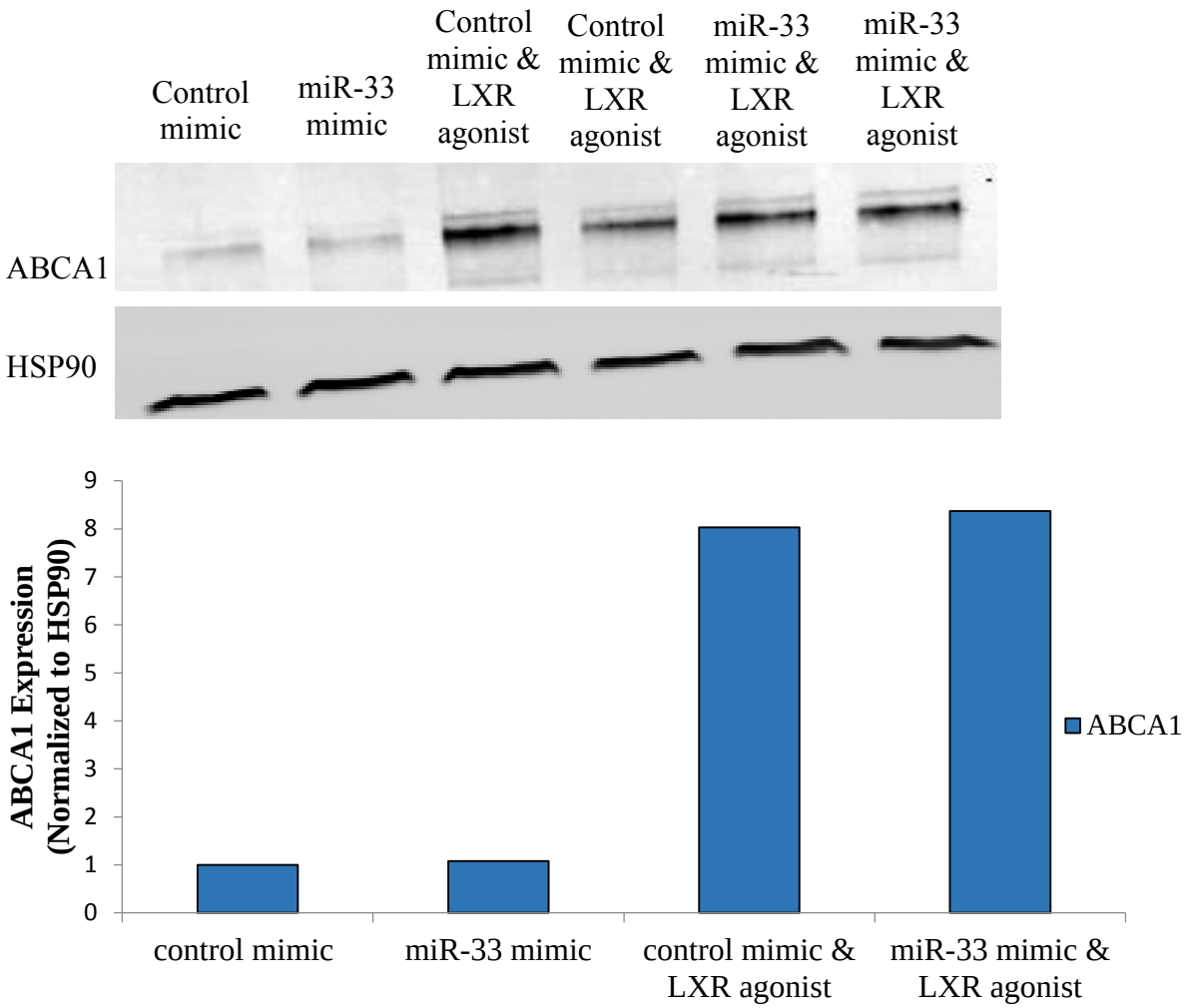

Figure 3.18. Protein expression of ABCA1 in BMDMs plated on a matrix containing 1μM of miR-33 mimic (+/- LXR agonist). ABCA1 expression was up-regulated after in BMDMs after 1 day of exposure to T0901317. Protein levels were examined by western blot analysis and normalised to HSP90. The experiment was n=1 and performed in duplicate.

DISCUSSION

4. Discussion

An understanding of the mechanism(s) by which matrix therapy functions in the treatment of MI is of utmost importance as it provides us with mechanistic insight, thus allowing us to target pathways that the matrix acts upon at a molecular level to enhance its therapeutic potential or reduce potential unwanted side effects. This study's first aim was to characterize whether a collagen matrix could regulate endogenous miRNAs and whether a miRNA mechanism may account, at least in part, for the beneficial functional effects observed in hearts treated with matrix at three hours post-MI. The matrix was found to down-regulate miR-21 expression in cardiac fibroblasts in culture, and 119 pre-miRNA and mature miRNAs were differentially expressed within the infarct and border zone in matrix-treated hearts. Of interest, the matrix was able to down-regulate miR-92a in post-MI infarct and peri-infarct tissue and in bone marrow-derived macrophages after 24 hours of culture on the matrix, offering insight into a potential mechanism by which the matrix confers its beneficial functional effects.

Since miR-21 is a highly expressed cardiac miRNA, and it has been shown to play a role in cardiac fibroblast activity and fibrosis,[44, 65] its regulation in fibroblasts by a collagen matrix was studied *in vitro*. The evaluation of miR-21 regulation by the matrix in cardiac fibroblasts was also pursued because matrix therapy delivered at 3 hours post-MI was shown to significantly reduce fibrosis and infarct size at 4 weeks after treatment (unpublished, N. Blackburn). Interestingly, 24 hours of culture on the matrix was able to down-regulate miR-21 in the fibroblasts, showing that the matrix is able to alter levels of endogenous miRNAs. Since the up-regulation of miR-21 in fibroblasts after MI is believed to contribute to fibrosis and that the therapeutic repression of miR-21 reduces fibrosis, it is possible that the decreased infarct size from matrix treatment could be a

result of the matrix down-regulating miR-21 thus leading to an up-regulation of Spry1 in fibroblasts. However the sample size needs to be increased to determine whether or not the matrix can significantly down-regulate miR-21 and up-regulate Spry1, a negative regulator of fibroblast survival and growth factor secretion. It is also possible that the matrix could be reducing fibrosis through a different miR-21 mediated pathway, such as the targeting of PTEN by miR-21.[44] To get a better understanding of how the matrix was regulating miRNAs *in vivo,* a miRNA microarray on cardiac tissue was performed.

Profiling of SHAM hearts and infarct and peri-infarct tissue in MI hearts 2 days after being treated with PBS or matrix (delivered at 3 hours post-MI) revealed that the matrix was able to regulate ~6% of endogenous miRNAs. The miRNA microarray did not indicate a significant difference in miR-21 levels between PBS and matrix-treated hearts. This could be related to the fact that the tissue was harvested at 2 days post-MI, which is not the infarct stage during which cardiac fibroblast proliferation and differentiation occurs. This stage occurs later during infarct evolution, beginning at about 5 days in mice; therefore if the tissue was harvested at a later date a difference in miR-21 expression might have been observed. Interestingly, miR-92a was significantly up-regulated after injury (in PBS-treated mice vs. SHAM), which correlated nicely with another study demonstrating that this miRNA is up-regulated after injury in a mouse model of MI.[74] The study also demonstrated that reducing miR-92a expression through the systemic administration of antagomiR-92a improved functional recovery of the damaged tissue 2 weeks after MI and augmented the number of capillaries and arterioles in the border zone.[74] These finding were of particular interest, as the matrix in the present study was able to significantly reduce miR-92a expression within the infarct and border zone after-MI. Notably, the matrix was able to achieve this without the use of therapeutic miRNAs, providing a novel alternative method to alter

endogenous miRNAs. In addition, the matrix increased the number of $CD31^+$ and SMA^+ vessels within the infarct and border zone and improved left ventricular ejection fraction at 4 weeks post-treatment (unpublished results, N. Blackburn). It was thus postulated that the down-regulation of miR-92a in matrix-treated hearts could be related to the beneficial function effects observed with matrix treatment, and so it was pursued for further study.

A well characterized role of miR-92a, is its anti-angiogenic function through the down-regulation of the endothelial protective and angiogenic integrin subunit α5 (ITGα5).[74, 75] Due to the fact that miR-92a was down-regulated and vascular density was increased in cardiac tissue after matrix treatment, potential miR-92a targets involved in angiogenesis were selected for further investigation: integrin subunit α5 (ITGα5), integrin subunit αV (ITGαV), ras-related protein Rap-1b (Rap-1b) and sphingosine-1-phosphate receptor 1 (S1P1).[92-96] The matrix significantly down-regulated ITGa5 and did not alter the expression of the other selected targets in cardiac tissue at 2 days post-treatment, which was opposite to the up-regulation that was expected. As miRNAs negatively regulate the translational output of target messenger RNA by translational repression and mRNA degradation, it is possible that miR-92a effects on ITGa5 are detectable at the protein level and not the mRNA level. Hickel et al. showed a down-regulation of ITGa5 at the protein level but not the mRNA level in the border zone of cardiac tissue after the localized down-regulation of miR-92a.[75] Furthermore, since the heart is multi-cellular, it is also possible that miR-92a is regulating ITGa5 and/or the other selected targets in a cell-specific manner, such as endothelial cells, which might not be detectable in multicellular samples.

Studies have demonstrated that that miR-92a over-expression in human endothelial cells causes a down-regulation of ITGa5, and that a matrix, similar to that used in this study, can up-regulate ITGaV and ITGa5 in circulating angiogenic cells (CACs) after 24h of culture.[33, 74, 97]

These findings indicate that a collagen-based matrix and miR-92a can regulate the expression of integrins, transmembrane receptors involved in cell-ECM interactions, within different types of vascular/angiogenic cells. Therefore, it was predicted that culturing CACs and HCAECs with the matrix would lead to the down-regulation of miR-92a and to the subsequent up-regulation of ITGaV and ITGa5. Unfortunately, matrix culture had no effect on miR-92a or ITGa5 and ITGaV levels within these two cell types in the culture conditions tested. Interestingly, miR-92a expression in CACs and HCAECs cultured on the matrix was slightly down-regulated, and ITGa5 protein levels in CACs after 4-day matrix culture was increased (although neither was significant) indicating that the matrix may be altering miR-92a expression in these cells, but not enough to cause a significant effect on its targets. This lack of regulation might be due to differences between the matrix used in this study and that used in the previously described work.[33] Specifically, the 2 matrix formulations used different cross-linkers (EDC/NHS vs. glutaraldehyde). Therefore, differences between the physical properties of the matrix due to different cross-linking could lead to these differences. Alternatively, variations in the cell isolation and culture conditions and techniques may also be contributing to the differences in integrin expression between the studies.

In situ hybridization has been used to show that miR-92a in 2 day post-MI tissue was present mostly in endothelial cells, but was also present in other cell types.[74] Since miR-92a is expressed in other cells present in the heart, miR-92a levels in cardiac fibroblasts and BMDMs cultured on a matrix was also analysed *in vitro*. Matrix culture had no effect on miR-92a expression in fibroblasts but it did cause its significant down-regulation in BMDMs, which could be contributing to the down-regulation observed *in vivo*.

The expression of mRNA for select miR-92a targets (ITGα5, ITGαV, Rap-1b) was un-altered in the BMDMs after 24h culture on the matrix. However, there was a trend (p=0.065) for

increased S1P1 mRNA expression in matrix-cultured BMDMs. It has been shown that S1P1 regulation alters the inflammatory phenotype of macrophages, with S1P1 activation limiting the expression of pro-inflammatory cytokines in macrophages.[98] This knowledge, and the fact that: 1) miR-92a targets S1P1; 2) the matrix down-regulated miR-92a in macrophages *in vitro*; and 3) there was a trend for the matrix to up-regulate S1P1 at the mRNA level in macrophages *in vitro*; and 4) the matrix altered macrophage polarization *in vivo* (unpublished, N. Blackburn), led me to further explore the expression of S1P1 in matrix-cultured macrophages. The protein level of S1P1 was examined in BMDMs cultured on the matrix for 24 hours and 3 days, and also in post-MI cardiac tissue treated with the matrix or PBS. In all these experiments, S1P1 protein levels were found to be un-altered. Therefore, miR-92a is most likely targeting mRNAs other than S1P1 in BMDMs, or S1P1 was not affected at the time-points examined. A role for miR-92a in macrophages and inflammation has been identified,[75-78, 99, 100] but more research is still necessary, particularly in elucidating the role of the ECM environment in regulating these processes. To help identify other potential miR-92a targets in BMDMs, online miRNA target databases need to be revisited. An emphasis should be placed on searching for targets involved in the regulation of inflammation, macrophage polarization, adhesion and ECM-cell interactions. In addition, although mRNA levels of ITGα5, ITGαV, Rap-1b were unchanged in these experiments, it remains to be determined if the same is observed for their protein levels. Even though its targets are yet to be identified, it is still likely that the matrix is down-regulating miR-92a in macrophages within the infarcted tissue to mediate the inflammatory response. Interestingly, other work in the Suuronen lab has shown that the matrix increases the M2 to M1 macrophage ratio within the infarct two days after matrix treatment (unpublished, N. Blackburn), which is the same time-point for which the miRNA microarray experiment was performed. Others have reported literature that miR-92a is down-

regulated in M2 macrophages,[78] so the down-regulation of miR-92a in the infarct of matrix-treated hearts could be associated with increased M2 macrophage numbers, which is important for cardiac repair. Based on this supporting evidence, it is possible that macrophages are contributing to the observed down-regulation of miR-92a *in vivo*.

Experiments studying the matrix effect on macrophage polarization would be necessary to confirm this hypothesis. Specifically, plating BMDMs on the matrix or a tissue culture plate and qPCR or staining for M1 and M2 markers could be performed to see if more M2 macrophages differentiated on the matrix. Furthermore, *in situ* hybridization for miR-92a in cardiac tissue sections could be performed in conjunction with M1 and M2 staining to compare macrophages and miRNA co-localization in matrix- and PBS-treated hearts.

A large number of macrophages are present in the infarct two days after MI.[13] Despite this, it is also possible that the matrix is regulating miR-92a in other cardiac cell types. The atheroprotective and angiogenic role of miR-92a reduction in endothelial cells has been well reported.[74-76, 100] The matrix is known to enhance angiogenesis;[33, 42, 90, 101] therefore, it is possible that the matrix is regulating miR-92a within endothelial and/or angiogenic cells *in vivo* and acting on ItgaV, Itga5, Rap1b and/or S1P1 to but with the help of specific environmental factors that aren't present *in vitro*. For instance, the matrix could be regulating the exosomal release of miR-92a from macrophages which could be altering endogenous levels in endothelial cells to cause angiogenic effects. To test this hypothesis, miR-92a content in exosomes from BMDMs plated on a matrix could be analyzed in comparison to a control. Conditioned media from matrix-cultured macrophages could also be placed on endothelial cells to see if it altered miR-92a levels. The expression of miR-92a and its angiogenic targets should also be examined in a co-culture experiment to see if their expression profile is altered in ECs when cultured with BMDMs.

It is also important to note that studying *in vivo* results *in vitro* is challenging since *in vivo* systems are complex and hard to mimic *in vitro*.[102] For instance, *in vitro* cellular profiles (M1/M2 macrophage phenotypes) will not necessarily mimic *in vivo* profiles.[102] Matrix and cellular interactions also vary between these two models. In the present study, the cells were plated on top of the matrix *in vitro*, whereas *in vivo*, the cells could be completely surrounded by the matrix or in close proximity to other cells interacting with the matrix (dependent on injection location and matrix dispersal). To confirm that the matrix is altering intracellular levels of miR-92a in macrophages and endothelial cells within the infarct, *in situ* hybridization for miR-92a would need to be performed in 3h- and 2-day post-treatment matrix- and PBS-treated tissue. Cell sorting by FACS analysis or magnetic beads could also be used to separate cardiac cell types from the infarct and border zone post-MI and utilized for cell-specific miR-92a and target quantification; however, cell numbers and viability render this technique challenging. In summary, it is evident that the matrix treatment is altering the miRNA profile in MI hearts, and it is improving the post-myocardial environment and function of the heart after MI. Several promising candidate miRNAs have been identified that may be involved in mediating the beneficial matrix effects, but the underlying mechanisms still remain to be determined.

In the second aim of this study, the matrix was tested as a novel strategy to deliver miRNA therapeutics. This was assessed as it could potentially address a number of challenges that are currently limiting the efficacy of delivery and the success of miRNA therapies. First, the matrix could serve to protect the therapeutic miRNA from the immune response and nucleases during delivery preventing them from being degraded and thus increasing the efficiency of the therapeutic. Second, it would allow the therapeutic miRNA to be locally delivered to the infarcted tissue, as the matrix is retained in the injection site, thus minimizing off-target effects. For these

reasons, the use of the biomaterial for miRNA delivery is extremely exciting. If the matrix could deliver miRNA therapeutics, the beneficial effect of matrix treatment could be further enhanced by up-regulating cardio-protective miRNAs or down-regulating harmful ones. The results presented in this thesis have not proven that the matrix is able to deliver functional therapeutic miRNAs to cells; however, some experiments showed promise, and further optimization is required.

Initially, the delivery potential of the matrix was assessed using a miRNA mimic for a miR-39, which is only expressed in *c. elegans.* Copies of cel-miR-39 were detectable in THP-1 cells and fibroblasts after being plated on a matrix containing the mimics. In addition, the number of copies detected in the samples was positively correlated with the concentration of mimics plated in the matrix. This highlighted the possibility that the amount of mimic delivered to the surrounding cells could be controlled by varying the concentration mixed into the matrix. This is important as a relation between the concentration of delivered anti-miRNAs *in vivo* has been associated with miRNA repression in off-target effects.[75] Despite these promising findings, cel-miR-39 copies were detected within experimental negative controls (matrix only, cells only, cells & matrix and 10nM and 100nM cel-miR-39 matrix washes). The detection of mimics in the washing controls could be a result of contamination from the matrix dislodged during the process performed to mimic lifting the cells off the matrix. Therefore, it is unclear whether or not the miRNAs detected in the cells & cel-miR-39 matrix samples were intracellular or from within the matrix dislodged during the washing process. In addition, the presence of cel-miR-39 in samples that had never come in contact with the miRNA mimic was alarming and added further uncertainty as to whether or not the mimics had been taken up by the cells from the matrix. This technical issue was tackled with the use of TaqMan probes but was unable to be resolved.

Interestingly, the matrix was able to retain miRNAs within the matrix after being in a culture environment for 1.5 days. The ability of the matrix to retain miRNA therapeutics, to a certain extent, is important as it shows that the miRNA is being incorporated into the matrix and when delivered *in vivo* could minimize off-target effects and provide cells with miRNAs for an extended period of time.

The functionality of the miRNAs once delivered is of utmost importance. Since there were technical issues with the cel-miR-39 system, the matrix's potential to deliver miRNA mimics was tested with a second system. This consisted of a dual luciferase plasmid containing the 3'UTR of ABCA1 and miR-33 mimics; as ABCA1 is a well-known target of miR-33.[103] A 3'UTR luciferase assay was then used to detect a depression in luciferase activity when the miRNA binds to its target. When HEK293 cells were transfected with the plasmid and plated on a matrix containing miR-33 mimics, a 20% depression of luciferase activity was observed in comparison to the control, indicating that the matrix could be delivering functional miRNAs to the cells. Unfortunately, HEK293 viability on the matrix was reduced and highly variable, therefore the experiment was unable to be successfully repeated. The same experiment was repeated using other cell types: HELA cells, which also didn't fare well on the matrix, and fibroblasts and BMDMs, which were not successfully transfected.

Western blot analysis was then utilized to test whether or not the matrix was able to deliver miR-33 mimics to BMDMs to repress ABCA1 protein levels. This technique was selected as it would also be able to tell us if the miRNA was functional once delivered without relying on an efficient transfection protocol. A significant reduction of ABCA1 was not observed in BMDMs plated on a matrix containing 1μM of mimic for 2, 3 or 5 days. Also, 2.5μM of mimic and anti-miR-33 applied to BMDMs on matrix for 3 days had no effect on ABCA1 levels. ABCA1

stimulation with an LXR agonist was performed on cells plated on a mimic-enriched matrix since the = 3'UTR luciferase assay was promising. Despite the activation of ABCA1, a significant down-regulation was not observed when the miR-33 mimic was added. Although no observed significant differences were observed, it is important to note that most experiments were only performed once or twice. In addition, a visible reduction in the band size of ABCA1 in BMDMs plated on a matrix containing mimics was occasionally observed in a duplicate indicating that the matrix might be able to deliver miRNA mimics to cells, but further optimization is required. For instance the preparation of the solutions used to make the matrix should be reassessed in addition to miRNA incorporation in the matrix. The 5-day and LXR ligand experiment offered the most promise, thus protein turnover or time might be necessary for the detection of miRNA delivery and functionality and should be repeated.

A similar study, which delivered miRNAs with a collagen matrix demonstrated the relationship of crosslinking concentration with miRNA elution and miRNA doping concentration with the regulation of its target proteins.[88] Therefore, tests to determine the ideal cross-linking and miRNA concentration should be further explored. Encapsulation of the miRNA before being doped in the matrix to potentially improve cellular uptake and functionality could also prove promising.

5. Conclusion

In conclusion, this study showed that the matrix is capable of regulating endogenous miRNA levels *in vitro* and *in vivo.* Specifically, *in vitro* it was shown that the matrix was able to: 1) down-regulate fibroblast expression of miR-21; and 2) down-regulate miR-92a expression in

BMDMs. In addition, compared to PBS controls, matrix treatment delivered 3 hours post-MI significantly altered the *in vivo* expression of 119 pre-miRNAs and mature miRNAs in the infarct and border zone of cardiac tissue 2 days after treatment. The observed down-regulation of miR-92a was of particular interest, since therapeutically reduced miR-92a expression has been shown to reduce scar formation, improve vascularisation and increase cardiac function post-MI. The in vitro results in the present study, in addition to evidence in the literature, suggest that the beneficial effects observed after matrix treatment could result, in part, from the down-regulation of miR-92a in M2 macrophages. Matrix therapy could potentially be enhanced if it could concomitantly be used to deliver miRNA therapeutics. This ability was also explored in the present study. Although it was not confirmed that the matrix is able to deliver functional miRNAs to cells, the results obtained did show promise that this will be possible, but further optimization is required.

6. References

1. McBane JE, Sharifpoor S, Labow RS, Ruel M, Suuronen EJ and Santerre JP. Tissue engineering a small diameter vessel substitute: engineering constructs with select biomaterials and cells. *Current vascular pharmacology*. 2012;10:347-60.
2. Frangogiannis NG. The immune system and cardiac repair. *Pharmacological research : the official journal of the Italian Pharmacological Society*. 2008;58:88-111.
3. Fraccarollo D, Galuppo P and Bauersachs J. Novel therapeutic approaches to post-infarction remodelling. *Cardiovascular research*. 2012;94:293-303.
4. Kempf T, Zarbock A, Vestweber D and Wollert KC. Anti-inflammatory mechanisms and therapeutic opportunities in myocardial infarct healing. *Journal of molecular medicine*. 2012;90:361-9.
5. Pfeffer MA and Braunwald E. Ventricular remodeling after myocardial infarction. Experimental observations and clinical implications. *Circulation*. 1990;81:1161-72.
6. Frangogiannis NG. The mechanistic basis of infarct healing. *Antioxidants & redox signaling*. 2006;8:1907-39.
7. Sutton MGSJ and Sharpe N. Left Ventricular Remodeling After Myocardial Infarction : Pathophysiology and Therapy. *Circulation*. 2000;101:2981-2988.
8. Ben-Mordechai T, Palevski D, Glucksam-Galnoy Y, Elron-Gross I, Margalit R and Leor J. Targeting Macrophage Subsets for Infarct Repair. *Journal of cardiovascular pharmacology and therapeutics*. 2014.
9. Gordon S. Alternative activation of macrophages. *Nature reviews Immunology*. 2003;3:23-35.
10. Mantovani A, Sica A, Sozzani S, Allavena P, Vecchi A and Locati M. The chemokine system in diverse forms of macrophage activation and polarization. *Trends in immunology*. 2004;25:677-86.
11. Nahrendorf M, Pittet MJ and Swirski FK. Monocytes: protagonists of infarct inflammation and repair after myocardial infarction. *Circulation*. 2010;121:2437-45.
12. Nahrendorf M, Swirski FK, Aikawa E, Stangenberg L, Wurdinger T, Figueiredo JL, Libby P, Weissleder R and Pittet MJ. The healing myocardium sequentially mobilizes two monocyte subsets with divergent and complementary functions. *The Journal of experimental medicine*. 2007;204:3037-47.
13. Troidl C, Mollmann H, Nef H, Masseli F, Voss S, Szardien S, Willmer M, Rolf A, Rixe J, Troidl K, Kostin S, Hamm C and Elsasser A. Classically and alternatively activated macrophages contribute to tissue remodelling after myocardial infarction. *Journal of cellular and molecular medicine*. 2009;13:3485-96.
14. Harel-Adar T, Ben Mordechai T, Amsalem Y, Feinberg MS, Leor J and Cohen S. Modulation of cardiac macrophages by phosphatidylserine-presenting liposomes improves infarct repair. *Proceedings of the National Academy of Sciences of the United States of America*. 2011;108:1827-32.
15. Morimoto H, Takahashi M, Izawa A, Ise H, Hongo M, Kolattukudy PE and Ikeda U. Cardiac overexpression of monocyte chemoattractant protein-1 in transgenic mice prevents cardiac dysfunction and remodeling after myocardial infarction. *Circulation research*. 2006;99:891-9.
16. Leor J, Rozen L, Zuloff-Shani A, Feinberg MS, Amsalem Y, Barbash IM, Kachel E, Holbova R, Mardor Y, Daniels D, Ocherashvilli A, Orenstein A and Danon D. Ex vivo

activated human macrophages improve healing, remodeling, and function of the infarcted heart. *Circulation*. 2006;114:I94-100.
17. Marti HH. Angiogenesis--a self-adapting principle in hypoxia. *Exs*. 2005:163-80.
18. Lee SH, Wolf PL, Escudero R, Deutsch R, Jamieson SW and Thistlethwaite PA. Early expression of angiogenesis factors in acute myocardial ischemia and infarction. *The New England journal of medicine*. 2000;342:626-33.
19. Li J, Brown LF, Hibberd MG, Grossman JD, Morgan JP and Simons M. VEGF, flk-1, and flt-1 expression in a rat myocardial infarction model of angiogenesis. *The American journal of physiology*. 1996;270:H1803-11.
20. Ren G, Michael LH, Entman ML and Frangogiannis NG. Morphological characteristics of the microvasculature in healing myocardial infarcts. *The journal of histochemistry and cytochemistry : official journal of the Histochemistry Society*. 2002;50:71-9.
21. Dobaczewski M, Akrivakis S, Nasser K, Michael LH, Entman ML and Frangogiannis NG. Vascular mural cells in healing canine myocardial infarcts. *The journal of histochemistry and cytochemistry : official journal of the Histochemistry Society*. 2004;52:1019-29.
22. Prater DN, Case J, Ingram DA and Yoder MC. Working hypothesis to redefine endothelial progenitor cells. *Leukemia*. 2007;21:1141-9.
23. Carmeliet P. Angiogenesis in Health and Disease. *Nature Medicine*. 2003.
24. Urbich C and Dimmeler S. Endothelial progenitor cells: characterization and role in vascular biology. *Circulation research*. 2004;95:343-53.
25. Suuronen EJ, Kuraitis D and Ruel M. Improving cell engraftment with tissue engineering. *Seminars in thoracic and cardiovascular surgery*. 2008;20:110-4.
26. Ruel M, Song J and Sellke FW. Protein-, gene-, and cell-based therapeutic angiogenesis for the treatment of myocardial ischemia. *Molecular and cellular biochemistry*. 2004;264:119-31.
27. Segers VF and Lee RT. Biomaterials to enhance stem cell function in the heart. *Circulation research*. 2011;109:910-22.
28. Zhang Y, Thorn S, DaSilva JN, Lamoureux M, DeKemp RA, Beanlands RS, Ruel M and Suuronen EJ. Collagen-based matrices improve the delivery of transplanted circulating progenitor cells: development and demonstration by ex vivo radionuclide cell labeling and in vivo tracking with positron-emission tomography. *Circulation Cardiovascular imaging*. 2008;1:197-204.
29. Lam MT and Wu Joseph C. Biomaterial applications in cardiovascular tissue repair and regeneration. *Expert Review of Cardiovascular Therapy*. 2012;10:1039-1049.
30. Laflamme MA, Chen KY, Naumova AV, Muskheli V, Fugate JA, Dupras SK, Reinecke H, Xu C, Hassanipour M, Police S, O'Sullivan C, Collins L, Chen Y, Minami E, Gill EA, Ueno S, Yuan C, Gold J and Murry CE. Cardiomyocytes derived from human embryonic stem cells in pro-survival factors enhance function of infarcted rat hearts. *Nature biotechnology*. 2007;25:1015-24.
31. Guo HD, Wang HJ, Tan YZ and Wu JH. Transplantation of marrow-derived cardiac stem cells carried in fibrin improves cardiac function after myocardial infarction. *Tissue engineering Part A*. 2011;17:45-58.
32. Wei HJ, Chen CH, Lee WY, Chiu I, Hwang SM, Lin WW, Huang CC, Yeh YC, Chang Y and Sung HW. Bioengineered cardiac patch constructed from multilayered mesenchymal stem cells for myocardial repair. *Biomaterials*. 2008;29:3547-56.

33. Ahmadi A, McNeill B, Vulesevic B, Kordos M, Mesana L, Thorn S, Renaud JM, Manthorp E, Kuraitis D, Toeg H, Mesana TG, Davis DR, Beanlands RS, DaSilva JN, deKemp RA, Ruel M and Suuronen EJ. The role of integrin alpha2 in cell and matrix therapy that improves perfusion, viability and function of infarcted myocardium. *Biomaterials*. 2014;35:4749-58.
34. Yan J, Yang L, Wang G, Xiao Y, Zhang B and Qi N. Biocompatibility evaluation of chitosan-based injectable hydrogels for the culturing mice mesenchymal stem cells in vitro. *Journal of biomaterials applications*. 2010;24:625-37.
35. Leor J, Tuvia S, Guetta V, Manczur F, Castel D, Willenz U, Petnehazy O, Landa N, Feinberg MS, Konen E, Goitein O, Tsur-Gang O, Shaul M, Klapper L and Cohen S. Intracoronary injection of in situ forming alginate hydrogel reverses left ventricular remodeling after myocardial infarction in Swine. *Journal of the American College of Cardiology*. 2009;54:1014-23.
36. Ou L, Li W, Zhang Y, Wang W, Liu J, Sorg H, Furlani D, Gabel R, Mark P, Klopsch C, Wang L, Lutzow K, Lendlein A, Wagner K, Klee D, Liebold A, Li RK, Kong D, Steinhoff G and Ma N. Intracardiac injection of matrigel induces stem cell recruitment and improves cardiac functions in a rat myocardial infarction model. *Journal of cellular and molecular medicine*. 2011;15:1310-8.
37. Landa N, Miller L, Feinberg MS, Holbova R, Shachar M, Freeman I, Cohen S and Leor J. Effect of injectable alginate implant on cardiac remodeling and function after recent and old infarcts in rat. *Circulation*. 2008;117:1388-96.
38. Lindsey ML, Mann DL, Entman ML and Spinale FG. Extracellular matrix remodeling following myocardial injury. *Annals of medicine*. 2003;35:316-26.
39. Suuronen EJ, Veinot JP, Wong S, Kapila V, Price J, Griffith M, Mesana TG and Ruel M. Tissue-engineered injectable collagen-based matrices for improved cell delivery and vascularization of ischemic tissue using CD133+ progenitors expanded from the peripheral blood. *Circulation*. 2006;114:I138-44.
40. Abbott A. Cell culture: biology's new dimension. *Nature*. 2003;424:870-2.
41. Frederick JR, Fitzpatrick JR, 3rd, McCormick RC, Harris DA, Kim AY, Muenzer JR, Marotta N, Smith MJ, Cohen JE, Hiesinger W, Atluri P and Woo YJ. Stromal cell-derived factor-1alpha activation of tissue-engineered endothelial progenitor cell matrix enhances ventricular function after myocardial infarction by inducing neovasculogenesis. *Circulation*. 2010;122:S107-17.
42. Suuronen EJ, Zhang P, Kuraitis D, Cao X, Melhuish A, McKee D, Li F, Mesana TG, Veinot JP and Ruel M. An acellular matrix-bound ligand enhances the mobilization, recruitment and therapeutic effects of circulating progenitor cells in a hindlimb ischemia model. *FASEB journal : official publication of the Federation of American Societies for Experimental Biology*. 2009;23:1447-58.
43. Kuraitis D, Hou C, Zhang Y, Vulesevic B, Sofrenovic T, McKee D, Sharif Z, Ruel M and Suuronen EJ. Ex vivo generation of a highly potent population of circulating angiogenic cells using a collagen matrix. *Journal of molecular and cellular cardiology*. 2011;51:187-97.
44. Roy S, Khanna S, Hussain SR, Biswas S, Azad A, Rink C, Gnyawali S, Shilo S, Nuovo GJ and Sen CK. MicroRNA expression in response to murine myocardial infarction: miR-21 regulates fibroblast metalloprotease-2 via phosphatase and tensin homologue. *Cardiovascular research*. 2009;82:21-9.

45. Small EM, Frost RJ and Olson EN. MicroRNAs add a new dimension to cardiovascular disease. *Circulation*. 2010;121:1022-32.
46. Bartel DP. MicroRNAs: genomics, biogenesis, mechanism, and function. *Cell*. 2004.
47. Ambros V. The function of animal microRNAs. *Nature*. 2004.
48. Small EM and Olson EN. Pervasive roles of microRNAs in cardiovascular biology. *Nature*. 2011;469:336-42.
49. Najafi-Shoushtari SH, Kristo F, Li Y, Shioda T, Cohen DE, Gerszten RE and Naar AM. MicroRNA-33 and the SREBP host genes cooperate to control cholesterol homeostasis. *Science*. 2010;328:1566-9.
50. Valencia-Sanchez AM, Liu J., Hannon G.J.,2 and Parker, R. Control of translation and mRNA degradation by miRNAs and siRNAs. *Genes & development*. 2006.
51. Creemers EE, Tijsen AJ and Pinto YM. Circulating microRNAs: novel biomarkers and extracellular communicators in cardiovascular disease? *Circulation research*. 2012;110:483-95.
52. Pigati L, Yaddanapudi SC, Iyengar R, Kim DJ, Hearn SA, Danforth D, Hastings ML and Duelli DM. Selective release of microRNA species from normal and malignant mammary epithelial cells. *PLoS One*. 2010;5:e13515.
53. Kosaka N, Iguchi H, Yoshioka Y, Takeshita F, Matsuki Y and Ochiya T. Secretory mechanisms and intercellular transfer of microRNAs in living cells. *The Journal of biological chemistry*. 2010;285:17442-52.
54. Chen TS, Lai RC, Lee MM, Choo AB, Lee CN and Lim SK. Mesenchymal stem cell secretes microparticles enriched in pre-microRNAs. *Nucleic acids research*. 2010;38:215-24.
55. He Y, Huang C, Lin X and Li J. MicroRNA-29 family, a crucial therapeutic target for fibrosis diseases. *Biochimie*. 2013;95:1355-9.
56. Chen JF, Murchison EP, Tang R, Callis TE, Tatsuguchi M, Deng Z, Rojas M, Hammond SM, Schneider MD, Selzman CH, Meissner G, Patterson C, Hannon GJ and Wang DZ. Targeted deletion of Dicer in the heart leads to dilated cardiomyopathy and heart failure. *Proceedings of the National Academy of Sciences of the United States of America*. 2008;105:2111-6.
57. Albinsson S, Suarez Y, Skoura A, Offermanns S, Miano JM and Sessa WC. MicroRNAs are necessary for vascular smooth muscle growth, differentiation, and function. *Arteriosclerosis, thrombosis, and vascular biology*. 2010;30:1118-26.
58. van Rooij E, Sutherland LB, Liu N, Williams AH, McAnally J, Gerard RD, Richardson JA and Olson EN. A signature pattern of stress-responsive microRNAs that can evoke cardiac hypertrophy and heart failure. *Proceedings of the National Academy of Sciences of the United States of America*. 2006;103:18255-60.
59. Ikeda S, Kong SW, Lu J, Bisping E, Zhang H, Allen PD, Golub TR, Pieske B and Pu WT. Altered microRNA expression in human heart disease. *Physiological genomics*. 2007;31:367-73.
60. Meloni M, Marchetti M, Garner K, Littlejohns B, Sala-Newby G, Xenophontos N, Floris I, Suleiman MS, Madeddu P, Caporali A and Emanueli C. Local inhibition of microRNA-24 improves reparative angiogenesis and left ventricle remodeling and function in mice with myocardial infarction. *Molecular therapy : the journal of the American Society of Gene Therapy*. 2013;21:1390-402.

61. van Rooij E, Sutherland LB, Thatcher JE, DiMaio JM, Naseem RH, Marshall WS, Hill JA and Olson EN. Dysregulation of microRNAs after myocardial infarction reveals a role of miR-29 in cardiac fibrosis. *Proceedings of the National Academy of Sciences of the United States of America*. 2008;105:13027-32.
62. Schober A, Nazari-Jahantigh M, Wei Y, Bidzhekov K, Gremse F, Grommes J, Megens RT, Heyll K, Noels H, Hristov M, Wang S, Kiessling F, Olson EN and Weber C. MicroRNA-126-5p promotes endothelial proliferation and limits atherosclerosis by suppressing Dlk1. *Nat Med*. 2014;20:368-76.
63. Wang K, Lin ZQ, Long B, Li JH, Zhou J and Li PF. Cardiac hypertrophy is positively regulated by MicroRNA miR-23a. *The Journal of biological chemistry*. 2012;287:589-99.
64. Fiedler J and Thum T. MicroRNAs in myocardial infarction. *Arteriosclerosis, thrombosis, and vascular biology*. 2013;33:201-5.
65. Thum T, Gross C, Fiedler J, Fischer T, Kissler S, Bussen M, Galuppo P, Just S, Rottbauer W, Frantz S, Castoldi M, Soutschek J, Koteliansky V, Rosenwald A, Basson MA, Licht JD, Pena JT, Rouhanifard SH, Muckenthaler MU, Tuschl T, Martin GR, Bauersachs J and Engelhardt S. MicroRNA-21 contributes to myocardial disease by stimulating MAP kinase signalling in fibroblasts. *Nature*. 2008;456:980-4.
66. Hanafusa H, Torii S, Yasunaga T and Nishida E. Sprouty1 and Sprouty2 provide a control mechanism for the Ras/MAPK signalling pathway. *Nature cell biology*. 2002;4:850-8.
67. Casci T, Vinos J and Freeman T. Sprouty, an Intracellular Inhibitor of Ras Signalling. *Cell*. 1999;96:655-665.
68. Villar AV, Garcia R, Merino D, Llano M, Cobo M, Montalvo C, Martin-Duran R, Hurle MA and Nistal JF. Myocardial and circulating levels of microRNA-21 reflect left ventricular fibrosis in aortic stenosis patients. *International journal of cardiology*. 2013;167:2875-81.
69. Patrick D. Stress-dependent cardiac remodelling occurs in absence of miRNA-21 in mice. *The Journal of Clinical Investigation*. 2010.
70. Thum T, Chau N, Bhat B, Gupta SK, Linsley PS, Bauersachs J and Engelhardt S. Comparison of different miR-21 inhibitor chemistries in a cardiac disease model. *J Clin Invest*. 2011;121:461-2; author reply 462-3.
71. Bang C, Batkai S, Dangwal S, Gupta SK, Foinquinos A, Holzmann A, Just A, Remke J, Zimmer K, Zeug A, Ponimaskin E, Schmiedl A, Yin X, Mayr M, Halder R, Fischer A, Engelhardt S, Wei Y, Schober A, Fiedler J and Thum T. Cardiac fibroblast-derived microRNA passenger strand-enriched exosomes mediate cardiomyocyte hypertrophy. *J Clin Invest*. 2014.
72. Patrick DM, Kauppinen S, Van Rooij E and Olson EN. Response to Thum et al. *J Clin Invest*. 2011;121:462-463.
73. Ventura A, Young AG, Winslow MM, Lintault L, Meissner A, Erkeland SJ, Newman J, Bronson RT, Crowley D, Stone JR, Jaenisch R, Sharp PA and Jacks T. Targeted deletion reveals essential and overlapping functions of the miR-17~92 family of miRNA clusters. *Cell*. 2008;132:875-886.
74. Bonauer A, Carmona G, Iwasaki M, Mione M, Koyanagi M, Fischer A, Burchfield J, Fox H, Doebele C, Ohtani K, Chavakis E, Potente M, Tjwa M, Urbich C, Zeiher AM and Dimmeler S. MicroRNA-92a controls angiogenesis and functional recovery of ischemic tissues in mice. *Science*. 2009;324:1710-3.

75. Hinkel R, Penzkofer D, Zuhlke S, Fischer A, Husada W, Xu QF, Baloch E, van Rooij E, Zeiher AM, Kupatt C and Dimmeler S. Inhibition of MicroRNA-92a protects against ischemia/reperfusion injury in a large-animal model. *Circulation*. 2013;128:1066-75.
76. Wu W, Xiao H, Laguna-Fernandez A, Villarreal G, Jr., Wang KC, Geary GG, Zhang Y, Wang WC, Huang HD, Zhou J, Li YS, Chien S, Garcia-Cardena G and Shyy JY. Flow-Dependent Regulation of Kruppel-Like Factor 2 Is Mediated by MicroRNA-92a. *Circulation*. 2011;124:633-41.
77. Lai L, Song Y, Liu Y, Chen Q, Han Q, Chen W, Pan T, Zhang Y, Cao X and Wang Q. MicroRNA-92a negatively regulates Toll-like receptor (TLR)-triggered inflammatory response in macrophages by targeting MKK4 kinase. *The Journal of biological chemistry*. 2013;288:7956-67.
78. Zhang Y, Zhang M, Zhong M, Suo Q and Lv K. Expression profiles of miRNAs in polarized macrophages. *International journal of molecular medicine*. 2013;31:797-802.
79. van Rooij E. The art of microRNA research. *Circulation research*. 2011;108:219-34.
80. Krutzfeldt J, Rajewsky N, Braich R, Rajeev KG, Tuschl T, Manoharan M and Stoffel M. Silencing of microRNAs in vivo with 'antagomirs'. *Nature*. 2005;438:685-9.
81. Hutvagner G. Sequence-specific inhibition of small RNA function. *PLOS*. 2004.
82. Jorgensen S, Baker A, Moller S and Nielsen BS. Robust one-day in situ hybridization protocol for detection of microRNAs in paraffin samples using LNA probes. *Methods*. 2010;52:375-81.
83. van Rooij E, Marshall WS and Olson EN. Toward microRNA-based therapeutics for heart disease: the sense in antisense. *Circulation research*. 2008;103:919-28.
84. Haussecker D and Kay MA. miR-122 continues to blaze the trail for microRNA therapeutics. *Molecular therapy : the journal of the American Society of Gene Therapy*. 2010;18:240-2.
85. Broderick JA and Zamore PD. MicroRNA therapeutics. *Gene therapy*. 2011;18:1104-10.
86. Suh JS, Lee JY, Choi YS, Chung CP and Park YJ. Peptide-mediated intracellular delivery of miRNA-29b for osteogenic stem cell differentiation. *Biomaterials*. 2013;34:4347-59.
87. Muthiah M, Park IK and Cho CS. Nanoparticle-mediated delivery of therapeutic genes: focus on miRNA therapeutics. *Expert opinion on drug delivery*. 2013;10:1259-73.
88. Monaghan M, Browne S, Schenke-Layland K and Pandit A. A Collagen-based Scaffold Delivering Exogenous MicroRNA-29B to Modulate Extracellular Matrix Remodeling. *Molecular therapy : the journal of the American Society of Gene Therapy*. 2014;22:786-96.
89. Moorthi A, Vimalraj S, Avani C, He Z, Partridge NC and Selvamurugan N. Expression of microRNA-30c and its target genes in human osteoblastic cells by nano-bioglass ceramic-treatment. *International journal of biological macromolecules*. 2013;56:181-5.
90. Kuraitis D, Zhang P, Zhang Y, Padavan DT, McEwan K, Sofrenovic T, McKee D, Zhang J, Griffith M, Cao X, Musaro A, Ruel M and Suuronen EJ. A stromal cell-derived factor-1 releasing matrix enhances the progenitor cell response and blood vessel growth in ischaemic skeletal muscle. *European cells & materials*. 2011;22:109-23.
91. Murthy S. LXR/RXR activation enhances basolateral efflux of cholesterol in CaCo-2 cells. *The Journal of Lipid Research*. 2002;43:1054-1064.
92. Choi S, Lee SA, Kwak TK, Kim HJ, Lee MJ, Ye SK, Kim SH, Kim S and Lee JW. Cooperation between integrin 5 and tetraspan TM4SF5 regulates VEGF-mediated angiogenic activity. *Blood*. 2008;113:1845-1855.

93. Urbich C. Shear Stress-Induced Endothelial Cell Migration Involves Integrin Signaling Via the Fibronectin Receptor Subunits alpha5 and beta1. *Arteriosclerosis, thrombosis, and vascular biology*. 2002;22:69-75.
94. Brooks PC, Clark RA and Cheresh DA. Requirement of vascular integrin alpha v beta 3 for angiogenesis. *Science*. 1994;264:569-71.
95. Chrzanowska-Wodnicka M, Kraus AE, Gale D, White GC and VanSluys J. Defective angiogenesis, endothelial migration, proliferation, and MAPK signaling in Rap1b-deficient mice. *Blood*. 2007;111:2647-2656.
96. Wang S, Zhang Z, Lin X, Xu DS, Feng Y and Ding K. A polysaccharide, MDG-1, induces S1P1 and bFGF expression and augments survival and angiogenesis in the ischemic heart. *Glycobiology*. 2010;20:473-84.
97. Asahara T, Masuda H, Takahashi T, Kalka C, Pastore C, Silver M, Kearne M, Magner M and Isner JM. Bone Marrow Origin of Endothelial Progenitor Cells Responsible for Postnatal Vasculogenesis in Physiological and Pathological Neovascularization. *Circulation research*. 1999;85:221-228.
98. Hughes JE, Srinivasan S, Lynch KR, Proia RL, Ferdek P and Hedrick CC. Sphingosine-1-phosphate induces an antiinflammatory phenotype in macrophages. *Circulation research*. 2008;102:950-8.
99. Nilsson S, Moller C, Jirstrom K, Lee A, Busch S, Lamb R and Landberg G. Downregulation of miR-92a is associated with aggressive breast cancer features and increased tumour macrophage infiltration. *PLoS One*. 2012;7:e36051.
100. Loyer X, Potteaux S, Vion AC, Guerin CL, Boulkroun S, Rautou PE, Ramkhelawon B, Esposito B, Dalloz M, Paul JL, Julia P, Maccario J, Boulanger CM, Mallat Z and Tedgui A. Inhibition of MicroRNA-92a Prevents Endothelial Dysfunction and Atherosclerosis in Mice. *Circulation research*. 2014;114:434-43.
101. Giordano C, Thorn SL, Renaud JM, Al-Atassi T, Boodhwani M, Klein R, Kuraitis D, Dwivedi G, Zhang P, Dasilva JN, Ascah KJ, Dekemp RA, Suuronen EJ, Beanlands RS and Ruel M. Preclinical evaluation of biopolymer-delivered circulating angiogenic cells in a swine model of hibernating myocardium. *Circulation Cardiovascular imaging*. 2013;6:982-91.
102. Martinez FO and Gordon S. The M1 and M2 paradigm of macrophage activation: time for reassessment. *F1000prime reports*. 2014;6:13.
103. Rayner KJ, Suarez Y, Davalos A, Parathath S, Fitzgerald ML, Tamehiro N, Fisher EA, Moore KJ and Fernandez-Hernando C. MiR-33 contributes to the regulation of cholesterol homeostasis. *Science*. 2010;328:1570-3.

7. Appendix

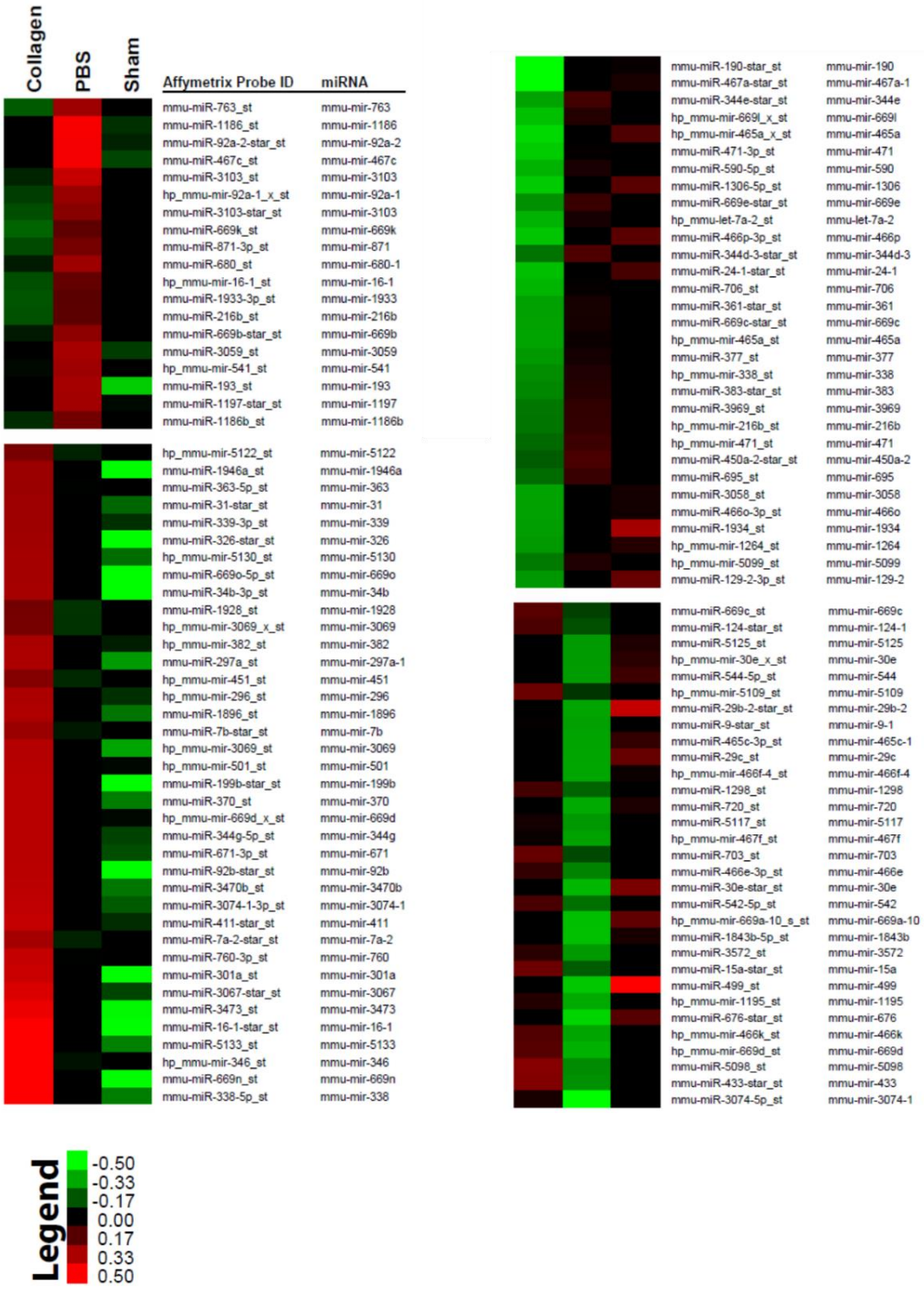
Collagen
PBS
Sham
Affymetrix Probe ID
miRNA
mmu-miR-763_st
mmu-mir-763
mmu-miR-1186_st
mmu-mir-1186
mmu-miR-92a-2-star_st
mmu-mir-92a-2
mmu-miR-467c_st
mmu-mir-467c
mmu-miR-3103_st
mmu-mir-3103
hp_mmu-mir-92a-1_x_st
mmu-mir-92a-1
mmu-miR-3103-star_st
mmu-mir-3103
mmu-miR-669k_st
mmu-mir-669k
mmu-miR-871-3p_st
mmu-mir-871
mmu-miR-680_st
mmu-mir-680-1
hp_mmu-mir-16-1_st
mmu-mir-16-1
mmu-miR-1933-3p_st
mmu-mir-1933
mmu-miR-216b_st
mmu-mir-216b
mmu-miR-669b-star_st
mmu-mir-669b
mmu-miR-3059_st
mmu-mir-3059
hp_mmu-mir-541_st
mmu-mir-541
mmu-miR-193_st
mmu-mir-193
mmu-miR-1197-star_st
mmu-mir-1197
mmu-miR-1186b_st
mmu-mir-1186b
hp_mmu-mir-5122_st
mmu-mir-5122
mmu-miR-1946a_st
mmu-mir-1946a
mmu-miR-363-5p_st
mmu-mir-363
mmu-miR-31-star_st
mmu-mir-31
mmu-miR-339-3p_st
mmu-mir-339
mmu-miR-326-star_st
mmu-mir-326
hp_mmu-mir-5130_st
mmu-mir-5130
mmu-miR-669o-5p_st
mmu-mir-669o
mmu-miR-34b-3p_st
mmu-mir-34b
mmu-miR-1928_st
mmu-mir-1928
hp_mmu-mir-3069_x_st
mmu-mir-3069
hp_mmu-mir-382_st
mmu-mir-382
mmu-miR-297a_st
mmu-mir-297a-1
hp_mmu-mir-451_st
mmu-mir-451
hp_mmu-mir-296_st
mmu-mir-296
mmu-miR-1896_st
mmu-mir-1896
mmu-miR-7b-star_st
mmu-mir-7b
hp_mmu-mir-3069_st
mmu-mir-3069
hp_mmu-mir-501_st
mmu-mir-501
mmu-miR-199b-star_st
mmu-mir-199b
mmu-miR-370_st
mmu-mir-370
hp_mmu-mir-669d_x_st
mmu-mir-669d
mmu-miR-344g-5p_st
mmu-mir-344g
mmu-miR-671-3p_st
mmu-mir-671
mmu-miR-92b-star_st
mmu-mir-92b
mmu-miR-3470b_st
mmu-mir-3470b
mmu-miR-3074-1-3p_st
mmu-mir-3074-1
mmu-miR-411-star_st
mmu-mir-411
mmu-miR-7a-2-star_st
mmu-mir-7a-2
mmu-miR-760-3p_st
mmu-mir-760
mmu-miR-301a_st
mmu-mir-301a
mmu-miR-3067-star_st
mmu-mir-3067
mmu-miR-3473_st
mmu-mir-3473
mmu-miR-16-1-star_st
mmu-mir-16-1
mmu-miR-5133_st
mmu-mir-5133
hp_mmu-mir-346_st
mmu-mir-346
mmu-miR-669n_st
mmu-mir-669n
mmu-miR-338-5p_st
mmu-mir-338
mmu-miR-190-star_st
mmu-mir-190
mmu-miR-467a-star_st
mmu-mir-467a-1
mmu-miR-344e-star_st
mmu-mir-344e
hp_mmu-mir-669l_x_st
mmu-mir-669l
hp_mmu-mir-465a_x_st
mmu-mir-465a
mmu-miR-471-3p_st
mmu-mir-471
mmu-miR-590-5p_st
mmu-mir-590
mmu-miR-1306-5p_st
mmu-mir-1306
mmu-miR-669e-star_st
mmu-mir-669e
hp_mmu-let-7a-2_st
mmu-let-7a-2
mmu-miR-466p-3p_st
mmu-mir-466p
mmu-miR-344d-3-star_st
mmu-mir-344d-3
mmu-miR-24-1-star_st
mmu-mir-24-1
mmu-miR-706_st
mmu-mir-706
mmu-miR-361-star_st
mmu-mir-361
mmu-miR-669c-star_st
mmu-mir-669c
hp_mmu-mir-465a_st
mmu-mir-465a
mmu-miR-377_st
mmu-mir-377
hp_mmu-mir-338_st
mmu-mir-338
mmu-miR-383-star_st
mmu-mir-383
mmu-miR-3969_st
mmu-mir-3969
hp_mmu-mir-216b_st
mmu-mir-216b
hp_mmu-mir-471_st
mmu-mir-471
mmu-miR-450a-2-star_st
mmu-mir-450a-2
mmu-miR-695_st
mmu-mir-695
mmu-miR-3058_st
mmu-mir-3058
mmu-miR-466o-3p_st
mmu-mir-466o
mmu-miR-1934_st
mmu-mir-1934
hp_mmu-mir-1264_st
mmu-mir-1264
hp_mmu-mir-5099_st
mmu-mir-5099
mmu-miR-129-2-3p_st
mmu-mir-129-2
mmu-miR-669c_st
mmu-mir-669c
mmu-miR-124-star_st
mmu-mir-124-1
mmu-miR-5125_st
mmu-mir-5125
hp_mmu-mir-30e_x_st
mmu-mir-30e
mmu-miR-544-5p_st
mmu-mir-544
hp_mmu-mir-5109_st
mmu-mir-5109
mmu-miR-29b-2-star_st
mmu-mir-29b-2
mmu-miR-9-star_st
mmu-mir-9-1
mmu-miR-465c-3p_st
mmu-mir-465c-1
mmu-miR-29c_st
mmu-mir-29c
hp_mmu-mir-466f-4_st
mmu-mir-466f-4
mmu-miR-1298_st
mmu-mir-1298
mmu-miR-720_st
mmu-mir-720
mmu-miR-5117_st
mmu-mir-5117
hp_mmu-mir-467f_st
mmu-mir-467f
mmu-miR-703_st
mmu-mir-703
mmu-miR-466e-3p_st
mmu-mir-466e
mmu-miR-30e-star_st
mmu-mir-30e
mmu-miR-542-5p_st
mmu-mir-542
hp_mmu-mir-669a-10_s_st
mmu-mir-669a-10
mmu-miR-1843b-5p_st
mmu-mir-1843b
mmu-miR-3572_st
mmu-mir-3572
mmu-miR-15a-star_st
mmu-mir-15a
mmu-miR-499_st
mmu-mir-499
hp_mmu-mir-1195_st
mmu-mir-1195
mmu-miR-676-star_st
mmu-mir-676
hp_mmu-mir-466k_st
mmu-mir-466k
hp_mmu-mir-669d_st
mmu-mir-669d
mmu-miR-5098_st
mmu-mir-5098
mmu-miR-433-star_st
mmu-mir-433
mmu-miR-3074-5p_st
mmu-mir-3074-1
Legend
-0.50
-0.33
-0.17
0.00
0.17
0.33
0.50

Figure 7.1. Heat map of altered miRNAs in infarct and peri-infarct tissue 2 days after treatment with a collagen matrix and PBS performed 3 hours after MI. miRNAs were sequenced in the cardiac tissue using the Affymetrix GeneChip miRNA Array. A heat map was constructed for the 89 mature miRNAs and 30 stem loop pre-miRNAs that had a fold-change greater than +/-0.3 $\log_2$ between the matrix and PBS treatment groups where green signified a down-regulation, red an up-regulation and black no alteration of the miRNA.

Mature miRNA or stem-loop	Fold change (matrix vs. PBS)	Target messenger RNA	Target Function
miR-758	-2.1	Tal1	Transcription factor with a role in angiogenesis
		ILK	Angiogenesis and survival
		Bcl2	Prevents apoptosis
miR-92a-1 (stem-loop)	-5.6	ITGα5	Cell-matrix communication, angiogenesis
		ITGαV	Cell-matrix communication, angiogenesis
		S1P1	Up-regulates FGF, promotes survival
		RAP1b	Role in integrin and VEGF signaling
miR-377	-2.4	VEGF	Major angiogenic cytokine
		IGF-1	Angiogenic cytokine
		Bcl2	Prevents apoptosis
		ITGαV	Cell-matrix communication, angiogenesis
miR-763	-2.7	ITGα5	Cell-matrix communication, angiogenesis
miR-375	-2.3	ITGβ1	Regulation of integrin-associated signaling
miR-466a-5p	-2.5	VEGF	Major angiogenic cytokine
miR-3572	2.1	Spred1 and Spred2	inhibit FGF signaling
miR-296 (stem-loop)	2	UNC5A	Pro-apoptotic
miR-433-5p	5.1	IL1-R and IL-1α	Activators of inflammation
miR-382 (stem-loop)	2	CCR5	Increases inflammatory response
		IFNγ	Activator of inflammation
		PTEN	Suppresses M1-to-M2 macrophage differentiation

Table 7.1. Top miRNA candidates regulated by the matrix after myocardial infarction. Ten miRNAs were selected for RT-qPCR validation with the use of online miRNA databases that identify target mRNA, pathways and the genomic location of a miRNA. The table indicates the fold-change of these miRNAs for matrix treatment vs. PBS treatment and the mRNA that they target with roles matching the functional benefit of the matrix.